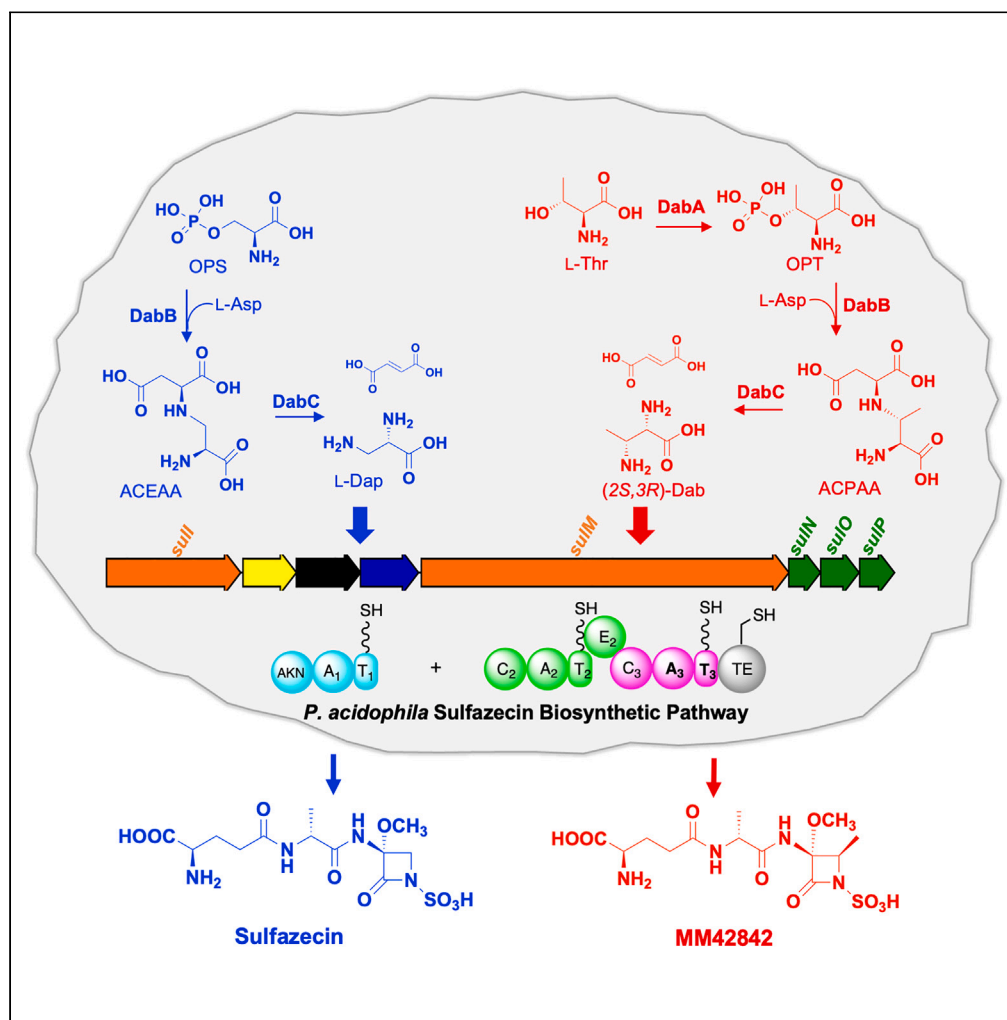


## Article

The *dabABC* operon is a marker of C4-alkylated monobactam biosynthesis and responsible for (2*S*,3*R*)-diaminobutyrate production

Rongfeng Li,  
Michael S.  
Lichstrahl, Trevor  
A. Zandi, Lukas  
Kahlert, Craig A.  
Townsend

ctownsend@jhu.edu

## Highlights

*DabABC* operons in natural product and monobactam BGCs biosynthesize (2*S*,3*R*)-Dab

Presence of the *dabABC* operon differentiates C4-methylated monobactam BGCs

Dual functions of DabB and DabC give (2*S*,3*R*)-Dab or L-Dap with/without L-Thr kinase

Results enable the enzymatic production of further functionalized Dap and Dab analogs

Li et al., iScience 27, 109202  
March 15, 2024 © 2024 The  
Author(s).  
[https://doi.org/10.1016/  
j.isci.2024.109202](https://doi.org/10.1016/j.isci.2024.109202)

## Article

The *dabABC* operon is a marker of C4-alkylated monobactam biosynthesis and responsible for (2*S*,3*R*)-diaminobutyrate productionRongfeng Li,<sup>1,5</sup> Michael S. Lichstrahl,<sup>1,3,5</sup> Trevor A. Zandi,<sup>2,4</sup> Lukas Kahlert,<sup>1</sup> and Craig A. Townsend<sup>1,6,\*</sup>

## SUMMARY

**Non-ribosomal peptide synthetases (NRPSs) assemble metabolites of medicinal and commercial value. Both serine and threonine figure prominently in these processes and separately can be converted to the additional NRPS building blocks 2,3-diaminopropionate (Dap) and 2,3-diaminobutyrate (Dab). Here we bring extensive bioinformatics, *in vivo* and *in vitro* experimentation to compose a unified view of the biosynthesis of these widely distributed non-canonical amino acids that both derive by pyridoxal-mediated  $\beta$ -elimination of the activated O-phosphorylated substrates followed by  $\beta$ -addition of an amine donor. By examining monobactam biosynthesis in *Pseudomonas* and in *Burkholderia* species where it is silent, we show that (2*S*,3*R*)-Dab synthesis depends on an L-threonine kinase (DabA), a  $\beta$ -replacement reaction with L-aspartate (DabB) and an argininosuccinate lyase-like protein (DabC). The growing clinical importance of monobactams to both withstand Ambler Class B metallo- $\beta$ -lactamases and retain their antibiotic activity make reprogrammed precursor and NRPS synthesis of modified monobactams a feasible and attractive goal.**

## INTRODUCTION

The rise of  $\beta$ -lactam resistant Gram-negative bacteria has been classified as one of the world's most pressing clinical threats by both the US Centers for Disease Control and Prevention (CDC) and the World Health Organization (WHO).<sup>1,2</sup> One particularly alarming mediator of this resistance is the emergence of Ambler Class B metallo- $\beta$ -lactamases (MBLs), which can inactivate most prescribed  $\beta$ -lactam antibiotics but for which no approved inhibitor currently exists. Only the monobactams with their unusual *N*-sulfamate possess an inherent stability to these enzymes.<sup>3</sup> This class of molecules, which was established with the discovery of the natural product sulfazecin (1),<sup>4</sup> has resulted in the FDA-approval of only one monobactam—aztreonam (2) (Figure 1B).<sup>5</sup>

Central to the biosynthesis of sulfazecin and other  $\beta$ -lactam antibiotics are members of the non-ribosomal peptide synthetase (NRPS) superfamily. These giant modular enzymes use the 20 common amino acids and select from among more than 500 specialized building blocks to assemble a vast array of secondary metabolites, many of which have important medical and commercial value. Biosynthetic innovations have evolved in core catalytic domains of these enzymes to modify certain amino acid substrates during peptide assembly to introduce new structural features in their products. Prominent among them are serine and threonine, which can be transformed to the  $\alpha,\beta$ -dehydroamino acid residues dehydroalanine and dehydrobutyrine,<sup>6,7</sup> respectively, and even create  $\beta$ -lactam rings embedded in their peptide products.<sup>8–10</sup> Prior to and separate from the action of NRPSs, both serine and threonine can be further modified to produce the additional NRPS building blocks 2,3-diaminopropionate (Dap) and 2,3-diaminobutyrate (Dab), respectively. The biosynthesis of these widely-distributed non-canonical amino acids has been addressed previously but many questions remain unanswered.

In sulfazecin biosynthesis, the gene couple responsible for producing L-Dap (3), *sulH* and *sulG*, is highly homologous to the characterized *sbnA*, a PLP-dependent cysteine synthase, and *sbnB*, a NAD<sup>+</sup> dependent dehydrogenase, genes from staphyloferrin biosynthesis as well as *cmnB* and *cmnK* from capreomycin biosynthesis, both of which have been previously characterized.<sup>11,12</sup> L-Dap is biosynthesized from the primary metabolites O-phosphoserine (OPS, 6) and L-glutamate (L-Glu), which are condensed in a PLP-dependent reaction to generate *N*-(2-amino-2-carboxyethyl) glutamic acid (ACEGA, 7). This intermediate then undergoes an NAD<sup>+</sup>-dependent oxidation/hydrolysis to efficiently generate 2-oxoglutarate (2OG, 8) and the L-Dap (3) product.<sup>11</sup>

<sup>1</sup>Department of Chemistry, The Johns Hopkins University, 3400 N Charles St, Baltimore, MD, USA

<sup>2</sup>T. C. Jenkins Department of Biophysics, The Johns Hopkins University, Baltimore, MD, USA

<sup>3</sup>Present address: Excet Inc., Springfield, VA, USA

<sup>4</sup>Present address: Novartis, Biomedical Research, Cambridge, MA, USA

<sup>5</sup>These authors contributed equally

<sup>6</sup>Lead contact

\*Correspondence: ctownsend@jhu.edu

<https://doi.org/10.1016/j.isci.2024.109202>



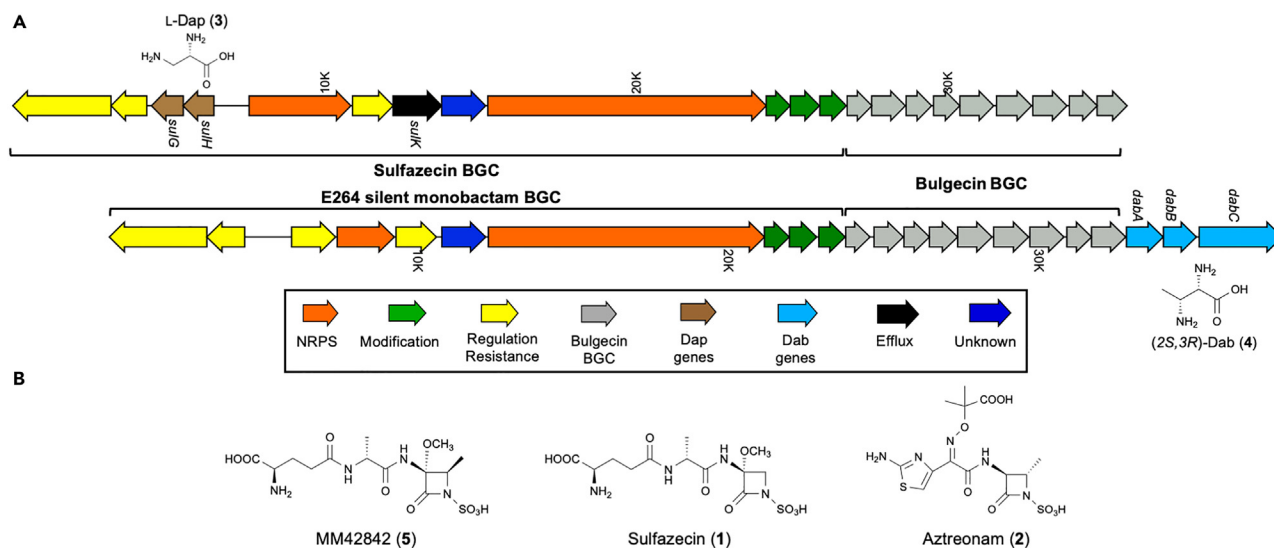


**Figure 1. Analysis of BGCs containing Dap and Dab operons**

(A) sulfazecin-bulgecin and the cryptic monobactam in *B. thailandensis* E264. *sulG-sulH* and *dabA-dabB-dabC* are operons responsible for the biosynthesis of L-Dap (3) and (2S,3R)-Dab (4), respectively.

(B) Structures of MM42842, sulfazecin, and aztreonam.

Aztreonam, and other synthetic monobactams that have been evaluated for clinical applications, differ importantly from naturally-occurring monobactams by the addition of a substituent at C-4 of the azetidinone ring, which has been demonstrated to improve both antimicrobial activity and stability to serine  $\beta$ -lactamases.<sup>13–15</sup> In sulfazecin biosynthesis, the carbon framework of the  $\beta$ -lactam is derived from the non-canonical  $\alpha,\beta$ -diamino acid L-Dap (3).<sup>16,17</sup> We have recently demonstrated that the sulfazecin biosynthetic machinery in *Pseudomonas acidophila* can accept  $\beta$ -branched derivatives of L-Dap (3), resulting in the production of methyl and fluoromethyl C-4 substituted monobactams by chemical complementation.<sup>18</sup> While in *P. acidophila* the *syn*-4-methyl-sulfazecin analogue arises from incorporation of the exogenously supplied amino acid (2S,3R)-diaminobutyrate (Dab, 4), this monobactam has also been isolated previously from *Pseudomonas cocovenans* and named MM42842 (5) (Figure 1B).<sup>19</sup>

Due to its altered antibacterial spectrum and  $\beta$ -lactamase-resistant properties, we were interested in investigating the biosynthetic origin of the C-4  $\beta$ -methyl group in naturally occurring MM42842 (5) as a prelude to introducing additional modifications at this site. Based on the detection of the same product in an L-Dap-deficient strain supplemented with (2S,3R)-Dab (4), we hypothesized that MM42842 (5) biosynthesis natively incorporates this amino acid as a precursor by an NRPS. There are numerous examples of other natural products that contain 2,3-Dab diastereomers as building blocks including friulimicin, pacidamycin, napsamycin, and mureidomycins.<sup>20–23</sup> In friulimicin biosynthesis, gene inactivation and substrate incorporation studies identified putative genes that were necessary for the production of (2S,3R)-Dab (4), implying that 2,3-Dab biosynthetic enzymes could be encoded in these biosynthetic gene clusters (BGCs),<sup>20,21</sup> although the enzymes have yet been identified and characterized.

MM42842 remains the only naturally occurring C-4 substituted monobactam and its biosynthesis has not been uncovered. Herein, we conducted extensive bioinformatics analysis to identify new monobactam BGCs that harbor putative genes responsible for Dab biosynthesis. The *in vivo* and *in vitro* experimentation enabled us to present a unified view for the first time that a tri-enzyme cascade encoded by the *dabABC* operon in a silent MM42842 producer is required to synthesize (2S,3R)-Dab (4). By examining monobactams and their biosynthetic intermediates produced in *Pseudomonas* and *in vitro* biochemical reactions, we also identified an unexpected crossover activity of DabB and DabC to generate L-Dap directly from OPS (6) in the absence of DabA. Overall, the *dabABC* operon was found to be a genomic signature for monobactam biosynthetic BGCs that synthesize C-4 methylated  $\beta$ -lactam rings. On the other hand, simpler unmethylated monobactams such as sulfazecin are characterized by BGCs that do not contain *dabABC*-like genes, but instead encode SulG and SulH homologues that lead to the conversion of OPS (6) to L-Dap in a mechanistically distinct way.

## RESULTS AND DISCUSSION

### Bioinformatic analysis of sulfazecin homologous gene clusters

We initially hoped to identify homologous genes to friulimicin *dabAB* and pacidamycin *pacQST* within the MM42842 BGC. Unfortunately, the MM42842-producing *P. cocovenans* strain has neither been sequenced nor is it accessible from any bacterial collection, leaving the identity of putative Dab biosynthetic genes in the MM42842 BGC unknown. Based on our hypothesis that activation of L-Thr as O-phospho-threonine (OPT, 9) is a requirement for activity of the PLP-dependent cysteine synthase homologue, we reasoned that the presence of an L-Thr kinase within a monobactam gene cluster would identify a producer of a C4-methyl monobactam such as MM42842 (5). To confirm our hypothesis,

**Table 1. BGCs containing L-Thr kinases genes and putative operons for biosynthesis of Dab or Dap**

Natural product	L-Threonine kinase	Dab or Dap Operons
Frulimicin	yes	DAB
Napsamycin	yes	DAB
Mureidomycin	yes	DAB
Pacidamycin	yes	DAB
Sulfazecin	No	DAP
Capreomycin	No	DAP
Staphyloferrin B	No	DAP
Viomycin	No	DAP
Edeine A	No	DAP

we searched a set of genomes of four known Dab and five known Dap producers with antiSMASH and indeed observed the presence of a putative L-Thr kinase consistently and exclusively in the Dab producers.<sup>24</sup> We thus re-examined a set of previously identified monobactam gene clusters<sup>16</sup> for an L-Thr kinase and several *Burkholderia* species were found that contained the anticipated kinase (Table 1).

We selected the *Burkholderia thailandensis* E264 monobactam BGC for further investigation. The overall gene organization and its encoded monobactam and bulgecin biosynthetic enzymes are very similar to those of the sulfazecin producer (Figure 1). Therefore, it seemed reasonable to predict the product from this BGC is similar to sulfazecin. However, *sulK*, encoding an RND efflux outer membrane lipoprotein, is absent from the E264 monobactam cluster. The most significant further difference is the absence of the Dap biosynthetic genes *sulG* and *sulH* and the addition of a 3-gene operon (*dabABC*) located at the end of E264 bulgecin BGC (Figure 1). This split monobactam–bulgecin–*dabABC* organization is also observed throughout all *Burkholderia* species harboring both monobactam BGCs and L-Thr kinase genes (Figure S1).

The *dabABC* operon encodes proteins sharing similarities to kinases (~45/60, identity/similarity), PLP-dependent cysteine synthases (~45/60), and lyase family protein/ATP-grasp domain-containing proteins (~35/55), respectively. Similar operons are found in BGCs using 2,3-Dab as building blocks for other natural products such as frulimicin, napsamycin, and pacidamycin<sup>20,22</sup> (Figure S2A). Interestingly, the Dap and Dab operons are organized differently across these BGCs, especially with the DabC homologous enzymes expressed either as N- and C-terminal individual proteins or the N-terminal domains fused to the PLP-dependent cysteine synthases (Figures S2A and S2B). In the case of frulimicin, gene inactivation, and genetic complementation showed that *dabA* and *dabB*, encoding a cysteine synthase and an arginosuccinate lyase homologous to the C-terminal E264 DabC, are essential for frulimicin biosynthesis (Figure S2A). Chemical complementation revealed that (2*S*,3*R*)-Dab (4), but not (2*S*,3*S*)-Dab (10), could restore frulimicin production, suggesting the former stereoisomer is the product synthesized by the Dab operon.<sup>20</sup> Because of the high similarities to other Dab enzymes and tight association with monobactam BGCs, we proposed the *dabABC* operon is likely responsible for (2*S*,3*R*)-Dab (4) biosynthesis in *B. thailandensis* E264 even though the gene organization is different.

### The monobactam gene cluster in *B. thailandensis* E264 is silent

Isolation of monobactam antibiotics have never been reported from any *Burkholderia* strains. Deletion of a global negative regulator *scmR* in *B. thailandensis* E264 resulted in increased levels of transcription of a monobactam-like BGC, but the  $\beta$ -lactam product of the cluster has never been described.<sup>25,26</sup> We used three fermentation media with the WT E264 and the *scmR* deletion mutant of *B. thailandensis*  $\Delta$ *scmR* to examine if any monobactam is produced by these strains. Fermentation supernatants and cell-free extracts were analyzed by a sensitive  $\beta$ -lactam-specific nitrocefin assay in which  $\beta$ -lactamase expression is induced by the presence of a  $\beta$ -lactam.<sup>27</sup> However, no  $\beta$ -lactamase induction activity was detected by the assays over the entire course of the fermentations in all media tested, indicating that the monobactam BGC is silent in *B. thailandensis* (Figure S3A).

### Analysis of the role of *sulK* in *P. acidophila* and *B. thailandensis* E264

A gene homologous to sulfazecin *sulK* is not present in the silent monobactam BGC of E264. Thus, we were interested in whether *sulK* is involved in sulfazecin (1) production in *P. acidophila* and the absence of such a gene caused silence in E264. During our previous search for the bulgecin BGC using transposon mutagenesis, we generated two bulgecin-deficient mutants in *P. acidophila*  $\Delta$ *sulG*. The first mutant had Tn5 insertion in bulgecin biosynthetic gene *bule*.<sup>28</sup> To identify the second mutant, its genomic DNA (gDNA) was digested with restriction enzymes and probed with the kanamycin-resistance cassette from Tn5.<sup>16</sup> DNA sequencing analysis of the positive 5.0-kb *Bam*HI-digested fragment revealed that the Tn5 transposon had inserted into *sulK* of the sulfazecin BGC (Figures S4A and S4B). We grew the mutant in *P. acidophila* fermentation medium supplemented with 2 mM L-Dap (3) to chemically complement the *sulG* deficit. Both nitrocefin and bioassays showed that production of sulfazecin was still abolished in the  $\Delta$ *sulG*/*sulK*::Tn5 mutant, indicating that *sulK* is in fact essential for the biosynthesis of both bulgecins and sulfazecin in *P. acidophila* (Figure S4C). Next, we constructed two expression vectors to test if expression of *sulK* in the *B. thailandensis*  $\Delta$ *scmR* mutant could activate the silent BGC and result in production of monobactam. We observed that the

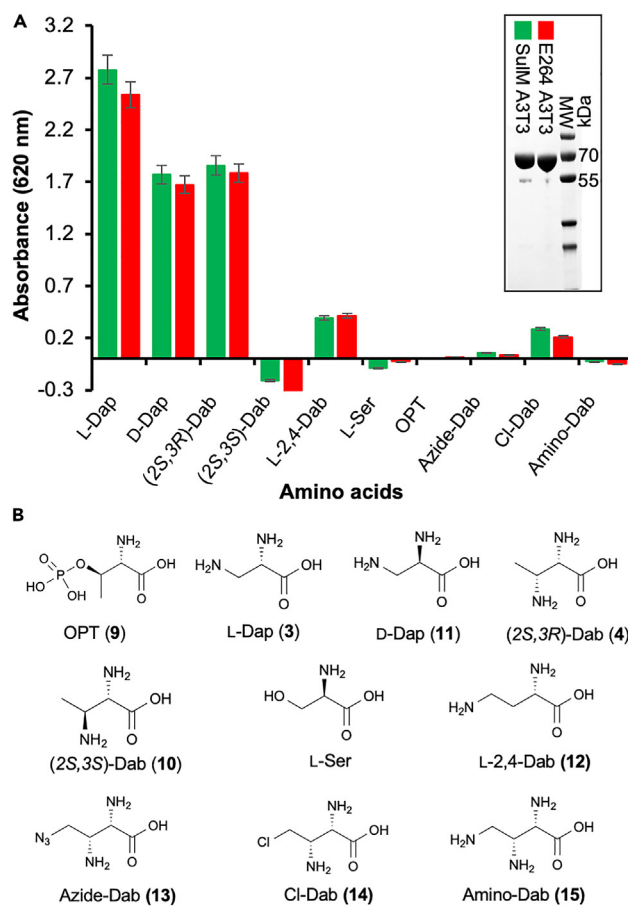


**Figure 2. Substrate specificity analysis of E264 A3T3 di-domain**

(A) A-domain substrate specificity *in vitro* assays of SulM A3T3 (green bars) and E264 A3T3 (red bars). The purified proteins of SulM A3T3 and E264 A3T3 are also shown.

(B) Amino acid substrates used in A-domain assays.

concentration of resistance to chloramphenicol increased to 70  $\mu\text{g}/\text{mL}$  in *B. thailandensis*  $\Delta\text{scmR}$  (pSCrhaB2Plus/Cm) when expression was induced with rhamnose compared to  $<5$   $\mu\text{g}/\text{mL}$  in uninduced clones, indicating that the  $P_{rha}$ BAD promoter is functional in *B. thailandensis*. Then we attempted to activate the silent monobactam cluster by expression of *sulK* in  $\Delta\text{scmR}$ . Five exconjugants of *B. thailandensis*  $\Delta\text{scmR}$  (pSCrhaB2Plus/*sulK*) were tested and two were also supplemented with 2 mM L-Dap (3) to the medium. However, no detectable  $\beta$ -lactam metabolites were observed based on nitrocefin assays from strains where expression of *sulK* was induced. This result suggested that either *sulK* may not be essential for monobactam biosynthesis in *B. thailandensis* or additional factors are required to activate the silent BGC (Figure S3B).

### A-domain substrate specificity of E264 A3

The large NRPS encoded in the E264 monobactam BGC showed  $\sim 80\%$  overall sequence similarity and share the same domain architecture as its counterpart SulM in the sulfazecin biosynthetic pathway.<sup>16</sup> Although A-domain bioinformatic analysis<sup>29,30</sup> failed to predict the amino acid activated by the last A-domain in the E264 large NRPS (E264 A3), the potential *dab* operon in its BGC and the results from previous chemical supplementation experiments in *P. acidophila*  $\Delta\text{sulG}$  suggested that (2S,3R)-Dab (4) could be the native substrate of E264 A3.<sup>18</sup> Therefore, the E264 A3T3 di-domain was expressed and used to analyze its substrate selectivity across several potential natural and synthetic amino acid substrates. As shown in Figure 2, colorimetric A-domain assays<sup>31</sup> showed that E264 A3T3 displayed a similar substrate selectivity and activity compared to SulM A3T3. It clearly activated (2S,3R)-Dab (4), L-Dap (3) and D-Dap (11), while no activation of (2S,3S)-Dab (10), L-Ser and OPT (9) and only slight activity with L-2,4-Dab (12) and three synthetic L-Dap analogs (13–15) was seen.<sup>18</sup> Interestingly, based on these endpoint assays E264 A3T3 actually seems to prefer L-Dap (3) over its proposed native substrate (2S,3R)-Dab (4), although E264 lacks the biosynthetic machinery (homologs to SulGH) to produce L-Dap (3) itself. To achieve a more detailed analysis, we applied the continuous 6-methyl-7-thioguanosine (MesG) hydroxylamine coupled assay<sup>32,33</sup> to determine the kinetic parameters of E264 A3T3 for both L-Dap (3) and (2S,3R)-Dab (4) (Figure S5). In agreement with relative activities and previous kinetic investigations of SulM A3T3,<sup>18</sup> the

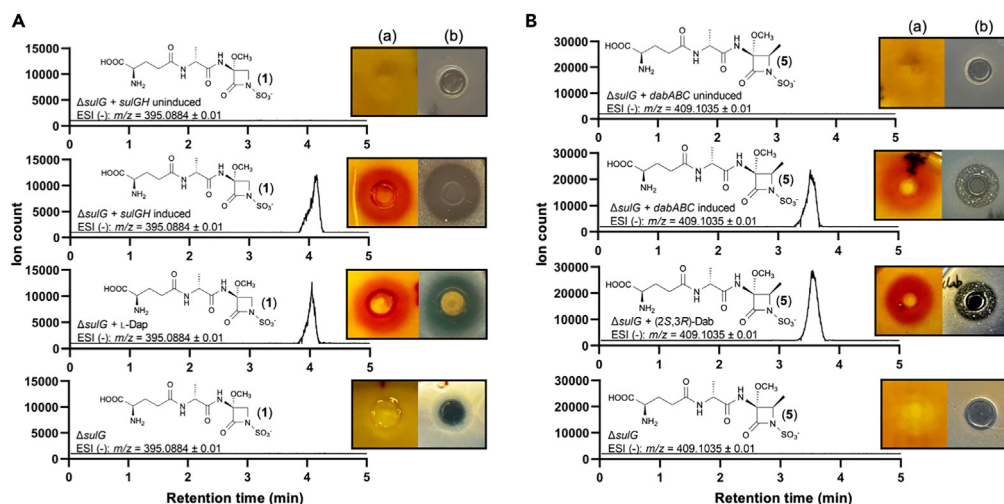


**Figure 3. Nitrocefin assays, bioassays, and UPLC-HRMS assays of *P. acidophila*  $\Delta$ *sulG* genetic and chemical complementation**

(A) *P. acidophila*  $\Delta$ *sulG* complemented by *sulGH* or L-Dap (3).

(B) *P. acidophila*  $\Delta$ *sulG* complemented by *dabABC* or (2*S*,3*R*)-Dab (4). (a). Nitrocefin assay. (b). Bioassay on *E. coli* ESS.

additional methyl-substituent in (2*S*,3*R*)-Dab (4) strongly increases  $K_M$  by approximately a factor of 10, whereas  $k_{cat}$  was only slightly diminished. Notably, E264 A3T3 exhibits an almost identical  $k_{cat}/K_M$  for L-Dap (3) (ca.  $85 \text{ mM}^{-1}\text{min}^{-1}$ ) and the larger (2*S*,3*R*)-Dab (4) ( $5.4 \text{ mM}^{-1}\text{min}^{-1}$ ) compared to SulM A3T3 (Figure S5).

### Genetic complementation of *P. acidophila* $\Delta$ *sulG* mutant and *in vivo* functional characterization of the *dabABC* operon

The previous *in vivo* chemical supplementation and *in vitro* A-domain assays showed that the sulfazecin biosynthetic pathway can incorporate both L-Dap (3) and (2*S*,3*R*)-Dab (4) as building blocks to produce sulfazecin (1) and MM42842 (5), respectively.<sup>18</sup> Next, we sought to see if the *P. acidophila*  $\Delta$ *sulG* mutant could be genetically complemented by expression of the *sulGH* operon. To achieve this goal, we first established a functional gene expression system in *P. acidophila*. Whole-genome DNA sequencing has suggested that many species including *P. acidophila* and the isosulfazecin producer *Pseudomonas mesoacidophila* previously attributed to genus *Pseudomonas* should be re-classified as genus *Burkholderia* or *Paraburkholderia*.<sup>28,34</sup> Thus, expression vectors and promoters developed for *Pseudomonas* may not actually be functional or genetically stable in these newly classified and untested species.<sup>35</sup> We examined three expression vectors pSCrhaB2Plus ( $P_{rhaBAD}$ ), pJM101( $P_{tac}$ ), and pUCU20-ANT2-MCS ( $P_{antA}$ ), that were all originally developed for gene expression in *P. aeruginosa*.<sup>36–38</sup> We found the  $P_{rhaBAD}$  and  $P_{tac}$  promoters were either not induced or only at very low activity as the expression of the chloramphenicol-resistance reporter gene did not result in elevated resistance to the antibiotic in the *P. acidophila*  $\Delta$ *sulGH* mutant (data not shown).

The expression vector pUCP20-ANT2-MCS contains an antranilate-inducible  $P_{antA}$  promoter that has been reported to be functional in a few *Pseudomonas* strains.<sup>39,38</sup> We used a similar approach as earlier in *B. thailandensis* to identify if the vector is fully functional in *P. acidophila* and found resistance to high concentrations of chloramphenicol in *P. acidophila*  $\Delta$ *sulG* (pUCP20-ANT2-MCS/*Cm*) achieved only when expression of the reporter gene was induced (Figure S6). The plasmid also appeared to be genetically stable in *P. acidophila*  $\Delta$ *sulG* as it could be maintained for several generations without losing the kanamycin selection marker and the re-isolated plasmids from multiple transformants showed no deletions or rearrangement by restriction digestions (data not shown). Therefore, these results indicated that the pUCP20-ANT2-MCS is fully functional in *P. acidophila*.

Then we tested if *sulG* could genetically complement the  $\Delta$ *sulG* mutant and restore production of sulfazecin. Surprisingly, growth inhibition bioassay, nitrocefin assay, and Ultra Performance Liquid Chromatography – High Resolution Mass Spectrometry (UPLC-HRMS) did not show sulfazecin (1) production when expression of *sulG* was induced in  $\Delta$ *sulG* (pUCP20-ANT2-MCS/*sulG*) cells. Sequence analysis revealed point mutations inside downstream *sulH* in the knockout mutant. These mutations appeared to be introduced by PCR during construction of the plasmid pEX18Km/FGmH<sup>16</sup> and introduced into the genome by homologous recombination causing the loss of activity of its encoded protein. To confirm our assumption, we cloned the *sulGH* operon into pUCP20-ANT2-MCS. Upon induction of *sulGH* expression with antranilate, we observed a sulfazecin (1) production in *P. acidophila*  $\Delta$ *sulG* (pUCP20-ANT2-MCS/*sulGH*) comparable to WT by bioassay, nitrocefin assay, and UPLC-HRMS. Thus, the genetic complementation revealed both *SulG* and *SulH* are inactive in *P. acidophila*  $\Delta$ *sulG* mutant. In addition, the overall sulfazecin (1) yields in the genetic complementation strain were comparable to those from the WT *P. acidophila* and *P. acidophila*  $\Delta$ *sulG* supplemented with L-Dap (3), indicating that the  $P_{antA}$  promoter is highly active and tightly controlled in *P. acidophila*, consistent with the results in other *Pseudomonas* strains (Figure 3A).<sup>38</sup>

Finally, to demonstrate if the *dabABC* operon in the silent in *B. thailandensis* E264 is responsible for the biosynthesis of (2*S*,3*R*)-Dab (4) *in vivo*, we constructed plasmid pUCP20-ANT2-MCS/*dabABC*, in which the expression of the *dabABC* operon was controlled by a single  $P_{antA}$

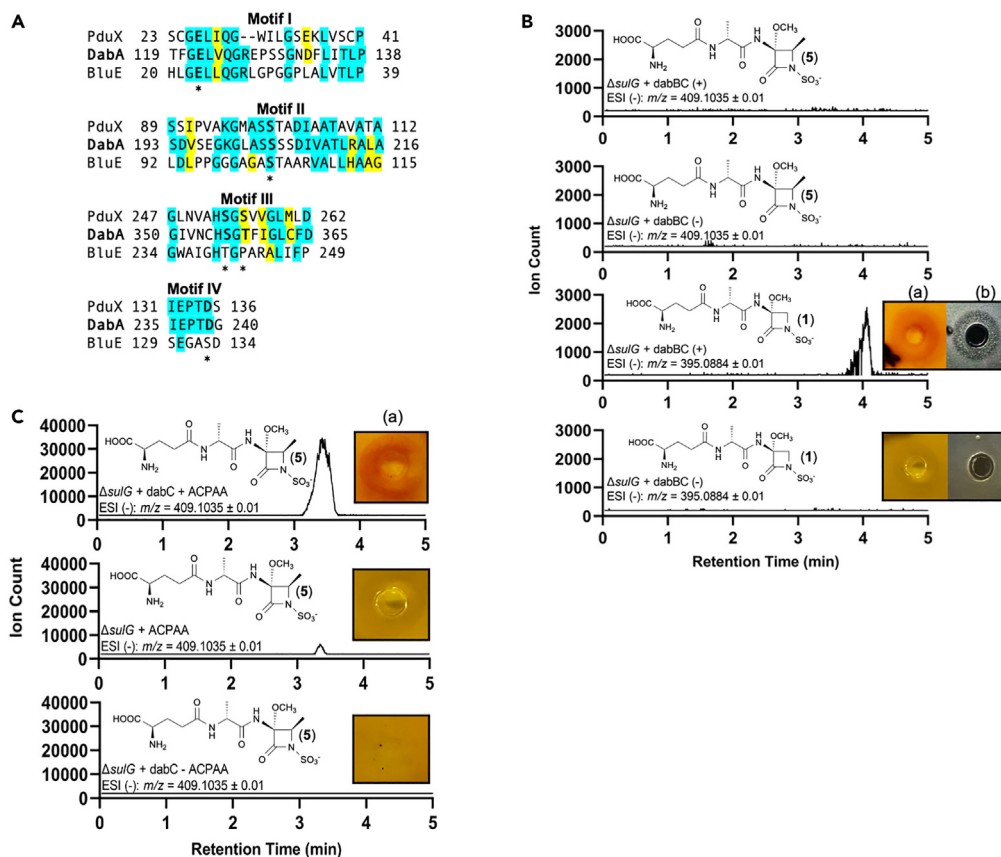


**Figure 4. In vivo characterization of DabA and DabC**

(A) Motifs I-III conserved in DabA and GHMP family kinases and Motif IV conserved in Pdux, BluE, and other L-Thr kinases. Identical and similar residues are highlighted in blue and yellow, respectively. Asterisks (\*) indicate residues demonstrated to be critical to enzyme activity. (B) Nitrocefin assays, bioassays, and UPLC-HRMS assays in *P. acidophila*  $\Delta sulG$  (pUCP20-ANT2-MCS/*dabBC*) showing sulfazecin (1) instead of MM42842 (5) was produced. (+) induced, (-) uninduced. (C) Nitrocefin assays, bioassays, and UPLC-HRMS assays of MM42842 (5) produced in *P. acidophila*  $\Delta sulG$  (pUCP20-ANT2-MCS/*dabC*) in the presence of 2 mM ACPAA (17),  $\Delta sulG$  supplemented with ACPAA (17), or induced *dabC* in  $\Delta sulG$  (pUCP20-ANT2-MCS/*dabC*) omitting of ACPAA (17). (a). Nitrocefin assay. (b). Bioassay on *E. coli* ESS.

promoter. Small but consistent inhibition zones on *E. coli* ESS and  $\beta$ -lactamase-induction activities on *B. licheniformis* were observed in cultures of *P. acidophila*  $\Delta sulG$  (pUCP20-ANT2-MCS/*dabABC*) when induced. These activities were elevated after the supernatants of fermentation were concentrated by 7x before conducting the assays. In contrast, the  $\Delta sulG$  mutant and uninduced cultures showed no antibacterial and  $\beta$ -lactamase-induction activities during the entire fermentation (Figure 3B). Therefore,  $\beta$ -lactam production was due to the induced expression of the *dabABC* operon. To further characterize the  $\beta$ -lactam product, the corresponding supernatants were partially purified before being analyzed by UPLC-HRMS. A mass corresponding to methyl-sulfazecin (MM42842, 5) was present in samples with expressed *dabABC*, but not in the mutant and uninduced controls. The mass and its retention time were identical to the MM42842 (5) produced from *P. acidophila*  $\Delta sulG$  with added (2S,3R)-Dab (4) (Figure 3B). In conclusion, the *in vivo* genetic complementation clearly demonstrated that the *dabABC* operon encodes enzymes responsible for (2S,3R)-Dab (4) biosynthesis.

### Functional characterization of DabA

Natural products friulimycin, napsamycin, and pacidamycin using either (2S,3R)-Dab (4) or (2S,3S)-Dab (10) as building blocks all harbor *dabA* homologs in their BGCs (Figure S2A; Table S1).<sup>20,21,40</sup> DabA showed relatively high sequence similarities to kinases from various prokaryotic species (~45/62). However, the two functionally characterized L-Thr kinases, PduX and BluE, in cobalamin biosynthesis, were not retrieved by BLASTP due to significant sequence differences among the members of this family of proteins.<sup>41,42</sup> Despite the low sequence similarity, alignment of DabA with PduX and BluE revealed DabA contains all four conserved motifs in L-Thr kinases. Motifs I, II, and III are conserved in all members of the GHMP kinase family<sup>43</sup> and probably involved in substrate (L-Thr) binding and interaction with the phosphates of ATP. The fourth conserved motif (Motif IV) is characteristic of PduX, BluE, and all other predicted but not experimentally verified L-Thr kinases, and

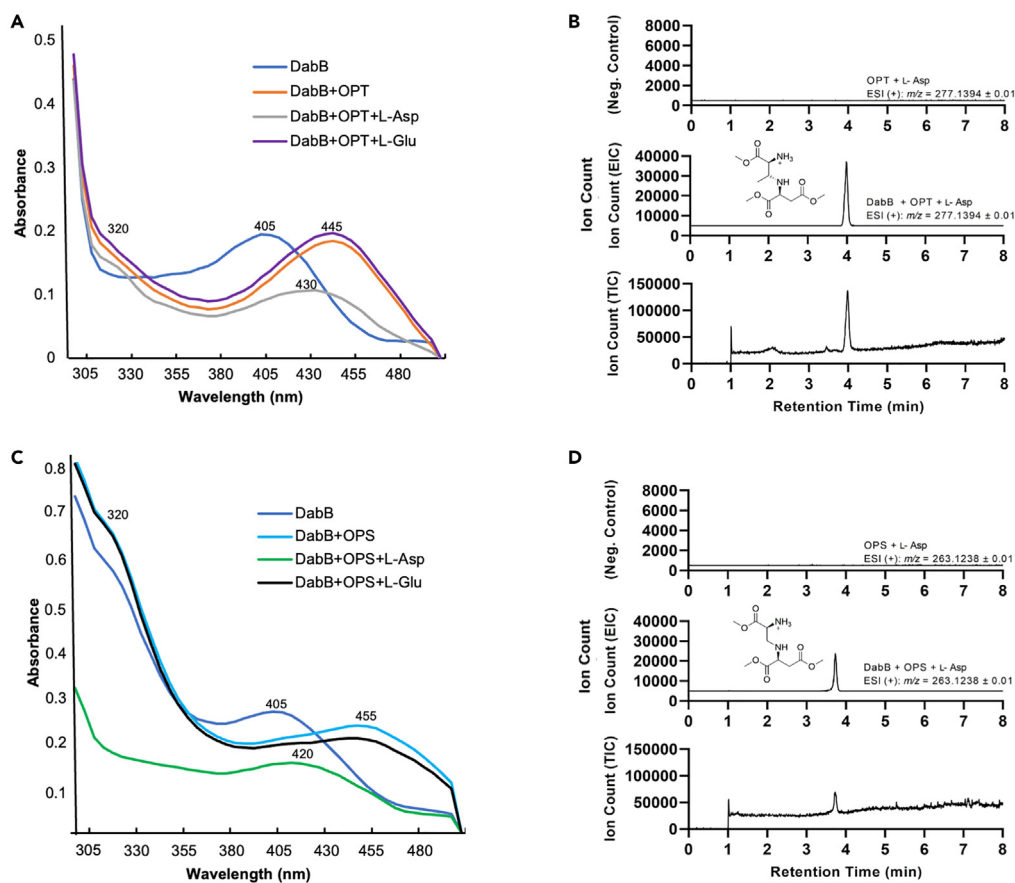


**Figure 5. In vitro characterization of DabB**

(A) UV-vis spectra of DabB, complex of DabB with OPT (9), and DabB-OPT with L-Asp or L-Glu. The wavelength of maximum absorbance is labeled. (B) UPLC-HRMS assays of ACPAA (17) trimethyl ester produced from OPT and L-Asp by DabB. (+): full reaction. (–): control reaction without DabB. (C) UV-vis spectra of DabB, complex of DabB with OPS (6), and DabB-OPS with L-Asp or L-Glu. The wavelength of maximum absorbance is labeled. (D) UPLC-HRMS assays of ACEAA (16) trimethyl ester produced from OPS and L-Asp by DabB. (+): full reaction. (–): control reaction without DabB.

is probably part of the active site or ATP-binding site.<sup>44</sup> In addition, the five amino acid residues previously demonstrated to be critical for PduX activity by site-specific mutagenesis are also all conserved in DabA<sup>44</sup> (Figure 4A).

*In vitro* characterization of DabA could not be carried out due to insolubility or insufficient quantities of soluble protein expressed in *E. coli*. PduX and BluE are involved in the biosynthetic salvage pathway of cobalamin.<sup>42</sup> Searching the *P. acidophila* genome for L-Thr kinases (DabA, PduX, or BluE) and other key enzymes of the pathway did not identify homologous proteins, further suggesting the absence of a cobalamin pathway and L-Thr kinases in this strain. To determine if DabA is essential for production of (2*S*,3*R*)-Dab (4), plasmid pUCP20-ANT2-MCS/*dabBC* was constructed and transformed into the  $\Delta$ *sulG* mutant to generate strain *P. acidophila*  $\Delta$ *sulG* (pUCP20-ANT2-MCS/*dabBC*). Aliquots of the supernatants were withdrawn after expression of *dabBC* was induced and partially purified before analysis by UPLC-HRMS to determine if MM42842 (5) was produced. As shown in Figure 4B, no MM42842 (5) was detected in  $\Delta$ *sulG* (pUCP20-ANT2-MCS/*dabBC*). The completely abolished production of MM42842 (5) associated with the absence of *dabA* revealed that DabA is essential for production of (2*S*,3*R*)-Dab (4). Therefore, combined with the bioinformatic analysis and DabB characterization (see below), this *in vivo* result strongly indicated that DabA is an L-Thr kinase that produces OPT (9) from L-Thr.

### Functional characterization of DabB

DabB and SulH are homologous to the class II PLP-dependent cysteine synthase enzymes and share ~36% amino acid similarity. We thus hypothesized that DabB catalyzes a similar reaction as SulH and SbnA.<sup>11,16</sup> Purified C-His<sub>6</sub> DabB shows a maximal absorbance at 405 nm due to the Schiff base formed between PLP and a lysine residue (Lys40) at the active site. The  $\lambda_{\text{max}}$  shifted to 320 and 445 nm when excess OPT (9) was mixed with the enzyme. OPS (6) also caused a spectral change to 320 and 455 nm when mixed with DabB. This absorption changes suggested that both OPT (11) and OPS (6) are used by DabB to form the analogous aminoacrylate intermediate coupled with phosphate release. L-Glu and L-Asp were then tested as coupling partners. We found the maximum absorbance moved to 430 nm when L-Asp, but not L-Glu, was added to DabB and OPT (9), indicating L-Asp is the exclusive amine donor to OPT (9)<sup>11</sup> (Figure 5A). Similarly, L-Asp also induced

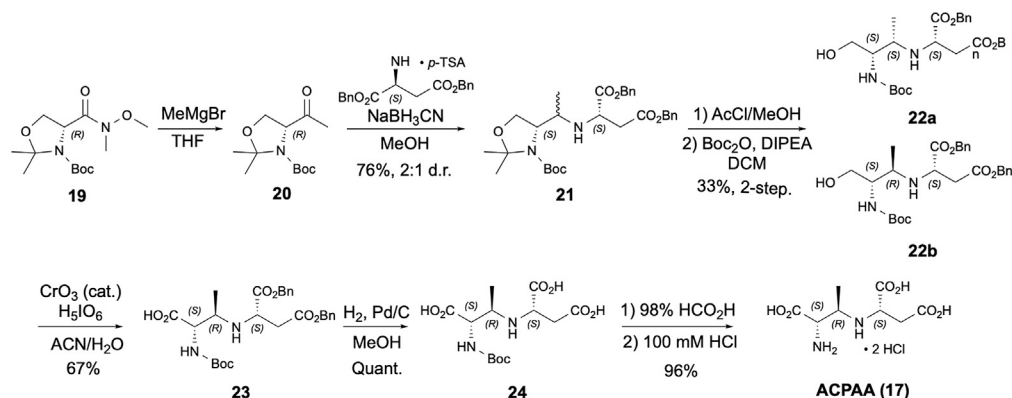


**Figure 6. Synthesis of ACPAA (17)**

a UV shift to 420 nm when mixed with DabB and OPS (6), but this shift was not observed when L-Glu was tested as amine donor, suggesting that L-Asp could be used with OPS (6) to form the addition product *N*-(2-amino-2-carboxylethyl) aspartic acid (ACEAA, 16, Figures 5C; Figure 7B). This result supports the results that DabB and DabC can produce L-Dap (3) *in vivo* when OPT (9) is not available in cells (see below).

The DabA and DabB analyses lead to the proposal that OPT (9) and L-Asp were likely the native substrates of DabB and form the product *N*-(1-amino-1-carboxy-2-propanyl) aspartic acid (ACPAA, 17) by linking the L-Thr β-carbon and L-Asp amine, while OPS (6) and L-Asp can be used as alternative substrates to produce ACEAA (16), similar as characterized in SulH and SbnA.<sup>11,16</sup> In order to directly detect and analyze the DabB product using UPLC-HRMS, we conducted *in vitro* DabB reactions and derivatized the mixtures by esterification in methanol<sup>45</sup> (Figure S8). As shown in Figures 5B and 5D, dominant mass ions at 277.14 and 263.124 were observed only in the full enzymatic reactions containing DabB, OPT (9) and L-Asp, and DabB, OPS (6), and L-Asp, respectively. They matched the predicted mass of ACPAA (17) and ACEAA (16) trimethyl esters and were not in the control reaction without DabB. No product was detected in reactions containing L-Glu as coupling amine donor, confirming that L-Glu is not used as substrate (data not shown). These data demonstrated that DabB can utilize either OPT (9) or OPS (6) as substrate to condense with L-Asp to produce ACPAA or ACEAA, respectively.

### Functional characterization of DabC

The modeled structure of DabC using AlphaFold<sup>46</sup> clearly showed two distinct domains (DabC-N and DabC-C) connected by a 16-aa linker (Figure S2B). The C-terminal domain showed structural similarity to known argininosuccinate lyases catalyzing the reversible breakdown of argininosuccinate to arginine and fumarate.<sup>47</sup> Despite this coupled arrangement, DabC-N and DabC-C are also expressed as individual proteins or fused to DabB homologues in other Dab operons<sup>20–22,40</sup> (Figure S2A), our *in vivo* genetic complementation data clearly showed the *holo* DabC functions to produce (2*S*,3*R*)-Dab (4) in concert with DabA and DabB.

To provide enough substrate for *in vitro* characterization of DabC, its proposed substrate ACPAA (17) was chemically synthesized (Figure 6). To prepare ACPAA (17), we initially hoped to use an approach similar to that of Hsu et al. in their synthesis of the intermediate ACEGA (7) from L-Dap (3) biosynthesis.<sup>12</sup> Using a cyclic sulfamidate (S1) derived from L-*allo*-Thr, we attempted to stereoselectively install the secondary amine by nucleophilic substitution with dibenzyl-L-aspartate (18) (Scheme S1). Although we previously found substitution with weakly basic, strong nucleophiles such as NaN<sub>3</sub> to be facile with this substrate,<sup>18</sup> the more basic, less nucleophilic amine of aspartate was not reactive. Only elimination byproduct was observed upon heating or extended reaction times. Reductive amination, on the other hand, is robust and selective<sup>48</sup> and has been used to form *N*-alkyl bonds in α-amino acids.<sup>49,50</sup>

To avoid potential racemization at the α-stereocenter in a threonine-derived ketone, we elected to use a methyl ketone-homologue (20)<sup>51</sup> to the well-known Garner aldehyde,<sup>52</sup> which could be readily prepared from protected D-serine (19, Figure 6).<sup>53</sup> Gratifyingly, reaction of 20 with dibenzyl-L-aspartate (18) and NaCNBH<sub>3</sub> generated the product 20 in good yield, albeit as a poorly separable ~2:1 mixture of diastereomers. Using the polar Felkin-Anh transition state model,<sup>54</sup> we expected the major diastereomer to be the desired 3*R*-stereochemistry. While some resolution of the diastereomers could be achieved by silica gel chromatography at this stage, we hoped that a later intermediate would prove easier to resolve. Thus, the mixture of 21 was subjected to acidic methanolysis to remove the acetonide group, followed by Boc re-protection. While this reaction sequence gave only modest yields, the two diastereomers 22a and 22b could be separated and characterized.

Diastereomerically pure 22b was then transformed to the carboxylic acid 23 by a catalytic Jones oxidation procedure.<sup>55</sup> Finally, hydrolysis of the esters and acidic *N*-deprotection, followed by anion exchange yielded ACPAA (17) as the dihydrochloride salt. <sup>1</sup>H-NMR analysis of this product showed H2-H3 vicinal coupling constant of 3.2 Hz, in line with our expectations for the 2*S*,3*R*-stereochemistry.<sup>18</sup>

Attempts to biochemically characterize DabC failed because of our inability to obtain soluble protein in sufficient amount. With the synthesized ACPAA (17) in hand, we developed an *in vivo* method as an alternative approach to analyze the function of DabC. A *dabC* expression vector, pUCP20-ANT2-MCS/*dabC*, was constructed and delivered into the Δ*sulG* mutant. Nitrocefin assay showed the appearance of induced β-lactamase activity from *P. acidophila* Δ*sulG* (pUCP20-ANT2-MCS/*dabC*) when expression of *dabC* was induced and supplemented

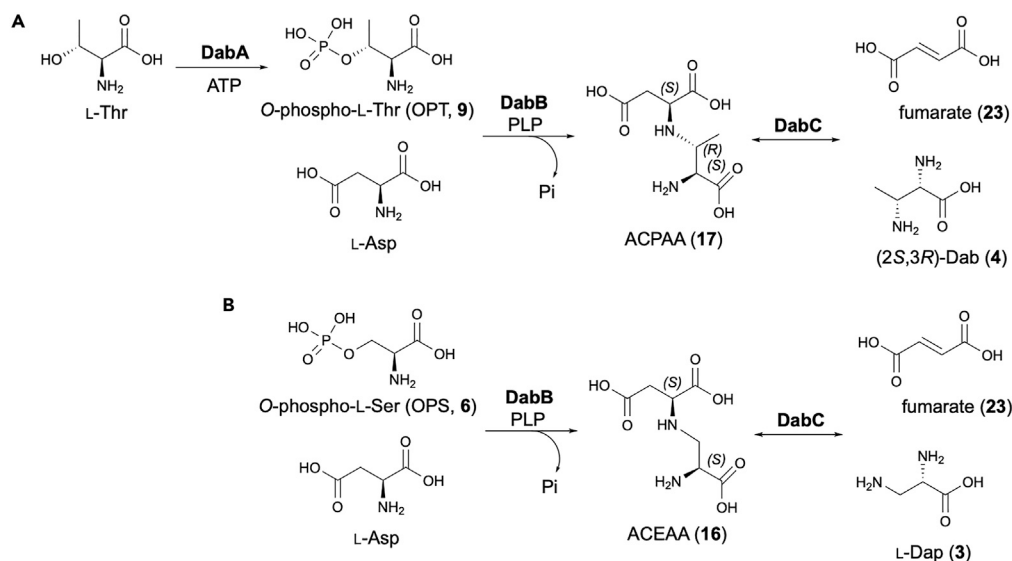


**Figure 7. The proposed Dab and Dap biosynthetic pathways**

(A) Proposed biosynthetic pathway to (2S,3R)-Dab (4) by DabA, DabB, and DabC.

(B) Proposed alternative biosynthetic pathway to L-Dap (3) by DabB and DabC.

with ACPAA (17). UPLC-HRMS analysis of the partially purified fermentation supernatant revealed the active product as MM42842 (5) (Figure 4C). No MM42842 (5) was detected when *dabC* expression was induced but ACPAA (17) was not added to the fermentation medium. In another control fermentation, a trace amount of MM42842 (5) was detected by UPLC-HRMS when 2 mM ACPAA (17) was administered directly to the  $\Delta$ *sulG* mutant (Figure 4C). The titer, however, was significantly less than that produced in the strain with induced *dabC* expression (<8% by ion count). The elimination of ACPAA (17) to yield (2S,3R)-Dab (4) and fumarate is a reversible reaction and, therefore, these species likely exist in equilibrium.<sup>47</sup> We had also observed decomposition of ACPAA (17) into (2S,3R)-Dab (4) and fumarate *in vitro* and hypothesized the leaking production of MM42842 (5) is due to the instability of ACPAA (17) under the acidic fermentation conditions of *P. acidophila* (pH 5.5–6.0). Collectively these data established that ACPAA (17) is the product of DabB and used by DabC to generate (2S,3R)-Dab (4) (Figure 4C).

### DabB and DabC can produce L-Dap from OPS and L-Asp

Although UPLC-HRMS analysis revealed MM42842 (5) was not produced in *P. acidophila*  $\Delta$ *sulG* (pUCP20-ANT2-MCS/*dabBC*), the bioassays and nitrocefin assays clearly showed production of a  $\beta$ -lactam product in the strain when both *dabB* and *dabC* were expressed. We partially purified the active product and analyzed it by UPLC-HRMS. To our surprise, UPLC-HRMS data clearly showed production of sulfazecin (1) in the induced strain, but not when *dabBC* expression had not been induced (Figure 4B). This deduction is also in agreement with the DabB *in vitro* result showing the enzyme can use OPS (6) and L-Asp as alternate substrates to generate ACEAA (16). The data from *dabBC* expression in *P. acidophila*  $\Delta$ *sulG* further indicated that ACEAA (16) produced by DabB can be cleaved by DabC to generate L-Dap (3). As OPT (9), OPS (6), and L-Asp all are available in  $\Delta$ *sulG* (pUCP20-ANT2-MCS/*dabABC*) genetic complementation cells, we were therefore interested to see if both MM42842 (5) and sulfazecin (1) are produced in this strain. Indeed, sulfazecin (1) was produced as the minor product in the strain when the UPLC-HRMS data of earlier fermentation samples were re-examined. Neither MM42842 (5) nor sulfazecin (1) was produced when expression of *dabABC* was not induced (Figure S7). We reasoned that the higher MM42842 (5) production could be due to OPT (9) being a better substrate of DabB than OPS (6) or the larger OPT (9) precursor pool produced by overexpressed *dabA* under the strong *P*<sub>antA</sub> promoter in  $\Delta$ *sulG* (pUCP20-ANT2-MCS/*dabABC*). In the event, this result indicated dual functions of DabB and DabC to produce (2S,3R)-Dab (4) from OPT and L-Asp and L-Dap (3) from OPS and L-Asp substrates.

Based on the *in vivo* and *in vitro* analyses of DabA, DabB, and DabC, the (2S,3R)-Dab (4) biosynthetic pathway and the proposed alternative functions of DabB, and DabC to produce L-Dap (3) are summarized in Figure 7. L-Dap (3) and 2,3-Dab are important non-canonical amino acids used as precursors to many natural products, some are of clinical importance. The absence of a threonine aldolase gene in *dabABC* operons in E264 silent monobactam BGCs is consistent with our chemical supplementation experiments and *in vitro* NRPS A-domain assays to demonstrate that (2S,3R)-Dab (4), not (2S,3S)-Dab (10) is the product of this three-gene operon. Our results clearly showed that the biosynthetic pathway begins similarly to L-Dap (3) by utilizing O-phosphorylated L-Ser or L-Thr, which are condensed with another amino acid as an amine donor in a PLP-dependent  $\beta$ -replacement reaction. However, rather than facilitating amine transfer by NAD<sup>+</sup> dependent oxidation/hydrolysis, DabC acts as a lyase to cleave this intermediate to release the final diamine product and fumarate. Our data, therefore, provide an alternative mechanism for the biosynthesis of L-Dap, where DabC can eliminate fumarate (23) from ACEAA (16) that is produced by DabB from OPS (6) as an alternative substrate. A previous investigation found enzyme activities in cell-free-extracts that produce Dab from L-Thr in a

mureidomycin producer. This study concluded that Dab was produced by a single PLP-dependent enzyme by a  $\beta$ -replacement reaction using ammonia as the nucleophile.<sup>56</sup> In contrast, when searching the BGC of the mureidomycin in *Streptomyces roseosporus*, we found a threonine aldolase-containing *dab*-like operon that is highly similar to those in napsamycin and pacidamycin BGCs<sup>57</sup> (Figure S2A), indicating that Dab biosynthesis in the mureidomycin pathway is functionally identical to (2S,3S)-Dab (10) in all these natural product producers.

Non-canonical amino acids can be incorporated into small molecules and proteins through non-ribosomal or semi-synthetic pathways and confer diversified architecture and bioactivity.<sup>58,59</sup> However, many of these non-canonical amino acids must be synthesized by chemo- or semi-synthetic methods often in low yield and under harsh reaction conditions as they are not naturally produced. Our discovery will enable further production of these compounds by environmentally- and cost-friendly methods. It also provides an opportunity for the enzymatic production of further functionalized analogues that could be incorporated into modified monobactams with improved antibiotic activity and resistance to metallo- $\beta$ -lactamases and other products. Finally, these discoveries will contribute to the discovery of new monobactam natural products by genome mining and guide their characterization.

### Limitations of the study

While the synthetic role of the L-threonine kinase DabA was established in this study, its *in vitro* production and demonstration of catalytic activity could not be directly shown despite protracted effort. The varied fusions and structures of DabA, B and C may affect through association or complex formation overall synthetic ability, which will require further experimentation to assess.

### STAR★METHODS

Detailed methods are provided in the online version of this paper and include the following:

- KEY RESOURCES TABLE
- RESOURCE AVAILABILITY
  - Lead contact
  - Materials availability
  - Data and code availability
- EXPERIMENTAL MODEL AND STUDY PARTICIPANT DETAILS
- METHOD DETAILS
  - Construction of recombinant plasmids
  - Generation and identification of *sulK* transposon mutant in *P. acidophila*
  - Protein expression and purification
  - Transformation, gene expression and fermentation of *B. thailandensis*
  - Transformation, gene expression and fermentation of *P. acidophila*
  - Detection of monobactam activities in *P. acidophila*
  - E264 and SulM A-domain pyrophosphate assay
  - Biochemical analysis of DabB
  - Synthesis of ACPAA
- QUANTIFICATION AND STATISTICAL ANALYSIS
- ADDITIONAL RESOURCES

### SUPPLEMENTAL INFORMATION

Supplemental information can be found online at <https://doi.org/10.1016/j.isci.2024.109202>.

### ACKNOWLEDGMENTS

This research was supported by NIH grant RO1 AI121072. We thank Professor T. Brüser, Leibniz University Hannover, for kindly providing expression vector pUCP20-ANT2-MCS. We thank Professor M. R. Seyedsayamdost, Princeton University, for generously providing *B. thailandensis* E264, *B. thailandensis*  $\Delta$ *scmR* and helpful discussion. We are pleased to acknowledge the help and guidance of Drs. I. P. Mortimer (ESI-MS) and J. Catazaró (NMR), Department of Chemistry. L.K. acknowledges financial support from the Deutsche Forschungsgemeinschaft – 492438365.

### AUTHOR CONTRIBUTIONS

R.F.L., M.S.L., T.A.Z., and C.A.T. conceived experiments and analyzed data. R.F.L., M.S.L., T.A.Z., L.K., and C.A.T. wrote the manuscript. R.F.L. carried out fermentation, vector construction, gene knockout, chemical and genetic complementation, protein expression and purification, and *in vitro* and *in vivo* product characterization and analyses. M.S.L. performed *in vitro* enzymatic analysis, derivatization of products, UPLC-HRMS analysis of *in vivo* and *in vitro* products, and synthesized ACPAA and Dabs. T.A.Z. carried out bioinformatic analysis, antiSMASH analysis, and DabB spectra and substrate analysis. L.K. carried out UPLC-HRMS analysis of *in vivo* and *in vitro* products, kinetic analysis of E264 A3T3 and synthesized ACPAA and Dabs.

## DECLARATION OF INTERESTS

The authors have no conflicts of interest.

Received: December 5, 2023

Revised: January 12, 2024

Accepted: February 7, 2024

Published: February 12, 2024

## REFERENCES

- Centers for Disease Control and Prevention (U.S.); National Center for Emerging Zoonotic and Infectious Diseases (U.S.); National Center for HIV/AIDS, STD, and TB Prevention (U.S.); National Center for Immunization and Respiratory Diseases (U.S.) (2013). Antibiotic resistance threats in the United States, 2013. April 23, 2013. <https://stacks.cdc.gov/view/cdc/20705>.
- World Health Organization (2023). Antimicrobial resistance surveillance in Europe - 2021 data (European Centre for Disease Prevention and Control and World Health Organization).
- Hinchliffe, P., Moreno, D.M., Rossi, M.A., Mojica, M.F., Martinez, V., Villamil, V., Spellberg, B., Drusano, G.L., Banchio, C., Mahler, G., et al. (2021). 2-Mercaptomethyl Thiazolidines (MMTZs) Inhibit All Metallo- $\beta$ -Lactamase Classes by Maintaining a Conserved Binding Mode. *ACS Infect. Dis.* 7, 2697–2706. <https://doi.org/10.1021/acscinfecdis.1c00194>.
- Sykes, R.B., Bonner, D.P., Bush, K., Georgopapadakou, N.H., and Wells, J.S. (1981). Monobactams - Monocyclic  $\beta$ -lactam antibiotics produced by bacteria. *J. Antimicrob. Chemother.* 8, 1–16. [https://doi.org/10.1093/jac/8.suppl\\_e.1](https://doi.org/10.1093/jac/8.suppl_e.1).
- Sykes, R.B., Bonner, D.P., Bush, K., and Georgopapadakou, N.H. (1982). Azthreonom (Sq 26,776), a synthetic monobactam specifically active against aerobic Gram-negative bacteria. *Antimicrob. Agents Chemother.* 21, 85–92. <https://doi.org/10.1128/Aac.21.1.85>.
- Wheaton, M.J., and Townsend, C.A. (2021). Evolutionary and functional analysis of an NRPS condensation domain integrates  $\beta$ -lactam, D-amino acid, and dehydroamino acid synthesis. *Proc. Natl. Acad. Sci. USA* 118, e2026017118. <https://doi.org/10.1073/pnas.2026017118>.
- Patteson, J.B., Fortinez, C.M., Putz, A.T., Rodriguez-Rivas, J., Bryant, L.H., 3rd, Adhikari, K., Weigt, M., Schmeing, T.M., and Li, B. (2022). Structure and function of a dehydrating condensation domain in nonribosomal peptide biosynthesis. *J. Am. Chem. Soc.* 144, 14057–14070. <https://doi.org/10.1021/jacs.1c13404>.
- Gaudelli, N.M., Long, D.H., and Townsend, C.A. (2015).  $\beta$ -Lactam formation by a non-ribosomal peptide synthetase during antibiotic biosynthesis. *Nature* 520, 383–387. <https://doi.org/10.1038/nature14100>.
- Long, D.H., and Townsend, C.A. (2018). Mechanism of integrated  $\beta$ -lactam formation by a nonribosomal peptide synthetase during antibiotic synthesis. *Biochemistry-US* 57, 3353–3358. <https://doi.org/10.1021/acs.biochem.8b00411>.
- Long, D.H., and Townsend, C.A. (2021). Acyl donor stringency and dehydroaminoacyl intermediates in  $\beta$ -Lactam formation by a non-ribosomal peptide synthetase. *ACS Chem. Biol.* 16, 806–812. <https://doi.org/10.1021/acschembio.1c00117>.
- Kobylarz, M.J., Grigg, J.C., Takayama, S.i.J., Rai, D.K., Heinrichs, D.E., and Murphy, M.E.P. (2014). Synthesis of L-2,3-diaminopropionic acid, a siderophore and antibiotic precursor. *Chem. Biol.* 21, 379–388. <https://doi.org/10.1016/j.chembiol.2013.12.011>.
- Hsu, S.H., Zhang, S., Huang, S.C., Wu, T.K., Xu, Z., and Chang, C.Y. (2021). Characterization of enzymes catalyzing the formation of the nonproteinogenic amino acid L-Dap in capreomycin biosynthesis. *Biochemistry-US* 60, 77–84. <https://doi.org/10.1021/acs.biochem.0c00808>.
- Sykes, R.B., and Bonner, D.P. (1985). Discovery and development of the monobactams. *Rev. Infect. Dis.* 7, S579–S593. [https://doi.org/10.1093/clinids/7.supplement\\_4.s579](https://doi.org/10.1093/clinids/7.supplement_4.s579).
- Carosso, S., Liu, R., Miller, P.A., Hecker, S.J., Glinka, T., and Miller, M.J. (2017). Methodology for monobactam diversification: syntheses and studies of 4-thiomethyl substituted  $\beta$ -lactams with activity against Gram-negative bacteria, including carbapenemase producing *Acinetobacter baumannii*. *J. Med. Chem.* 60, 8933–8944. <https://doi.org/10.1021/acs.jmedchem.7b01164>.
- Reck, F., Bermingham, A., Blais, J., Capka, V., Cariaga, T., Casarez, A., Colvin, R., Dean, C.R., Fekete, A., Gong, W., et al. (2018). Optimization of novel monobactams with activity against carbapenem-resistant *Enterobacteriaceae* – Identification of LYS228. *Bioorg. Med. Chem. Lett.* 28, 748–755. <https://doi.org/10.1016/j.bmcl.2018.01.006>.
- Li, R., Oliver, R.A., and Townsend, C.A. (2017). Identification and characterization of the sulfazecin monobactam biosynthetic gene cluster. *Cell Chem. Biol.* 24, 24–34. <https://doi.org/10.1016/j.chembiol.2016.11.010>.
- Oliver, R.A., Li, R., and Townsend, C.A. (2018). Monobactam formation in sulfazecin by a nonribosomal peptide synthetase thioesterase. *Nat. Chem. Biol.* 14, 5–7. <https://doi.org/10.1038/Nchembio.2526>.
- Lichstrahl, M.S., Kahlert, L., Li, R., Zandi, T.A., Yang, J., and Townsend, C.A. (2023). Synthesis of functionalized 2,3-diaminopropionates and their potential for directed monobactam biosynthesis. *Chem. Sci.* 14, 3923–3931. <https://doi.org/10.1039/d2sc06893a>.
- Box, S.J., Brown, A.G., Gilpin, M.L., Gwynn, M.N., and Spear, S.R. (1988). MM 42842, a new member of the monobactam family produced by *Pseudomonas cocovenenans*. II. Production, isolation and properties of MM 42842. *J. Antibiot.* 41, 7–12. <https://doi.org/10.7164/antibiotics.41.7>.
- Müller, C., Nolden, S., Gebhardt, P., Heinzlmann, E., Lange, C., Puk, O., Welzel, K., Wohlleben, W., and Schwartz, D. (2007). Sequencing and analysis of the biosynthetic gene cluster of the lipopeptide antibiotic friulimicin in *Actinoplanes friuliensis*. *Antimicrob. Agents Chemother.* 51, 1028–1037. <https://doi.org/10.1128/AAC.00942-06>.
- Zhang, W., Ostash, B., and Walsh, C.T. (2010). Identification of the biosynthetic gene cluster for the pacidamycin group of peptidyl nucleoside antibiotics. *Proc. Natl. Acad. Sci. USA* 107, 16828–16833. <https://doi.org/10.1073/pnas.1011557107>.
- Kaysser, L., Tang, X., Wemakor, E., Sedding, K., Hennig, S., Siebenberg, S., and Gust, B. (2011). Identification of a napsamycin biosynthesis gene cluster by genome mining. *Chembiochem* 12, 477–487. <https://doi.org/10.1002/cbic.201000460>.
- Jiang, L., Wang, L., Zhang, J., Liu, H., Hong, B., Tan, H., and Niu, G. (2015). Identification of novel mureidomycin analogues via rational activation of a cryptic gene cluster in *Streptomyces roseosporus* NRRL 15998. *Sci. Rep.* 5, 14111–14123. <https://doi.org/10.1038/srep14111>.
- Blin, K., Shaw, S., Augustijn, H.E., Reitz, Z.L., Biermann, F., Alanjary, M., Fetter, A., Terlouw, B.R., Metcalf, W.W., Helfrich, E.J.N., et al. (2023). antiSMASH 7.0: new and improved predictions for detection, regulation, chemical structures and visualisation. *Nucleic Acids Res.* 51, W46–W50. <https://doi.org/10.1093/nar/gkad344>.
- Guillouzer, L.S., Groleau, M.C., Mauffrey, F., and Déziel, E. (2020). ScmR, a global regulator of gene expression, quorum sensing, pH homeostasis, and virulence in *Burkholderia thailandensis*. *J. Bacteriol.* 202, e00776-19. <https://doi.org/10.1128/JB.00776-19>.
- Mao, D., Bushin, L.B., Moon, K., Wu, Y., and Seyedsayamdost, M.R. (2017). Discovery of scmR as a global regulator of secondary metabolism and virulence in *Burkholderia thailandensis* E264. *Proc. Natl. Acad. Sci. USA* 114, E2920–E2928. <https://doi.org/10.1073/pnas.1619529114>.
- O’Callaghan, C.H., Morris, A., Kirby, S.M., and Shingler, A.H. (1972). Novel method for detection of  $\beta$ -lactamases by using a chromogenic cephalosporin substrate. *Antimicrob. Agents Chemother.* 1, 283–288. <https://doi.org/10.1128/AAC.1.4.283>.
- Horsman, M.E., Marous, D.R., Li, R., Oliver, R.A., Byun, B., Emrich, S.J., Boggess, B., Townsend, C.A., and Mobashery, S. (2017). Whole-genome shotgun sequencing of two  $\beta$ -proteobacterial species in search of the bulgecin biosynthetic cluster. *ACS Chem. Biol.* 12, 2552–2557. <https://doi.org/10.1021/acschembio.7b00687>.
- Challis, G.L., Ravel, J., and Townsend, C.A. (2000). Predictive, structure-based model of

- amino acid recognition by nonribosomal peptide synthetase adenylation domains. *Chem. Biol.* 7, 211–224. [https://doi.org/10.1016/s1074-5521\(00\)00091-0](https://doi.org/10.1016/s1074-5521(00)00091-0).
30. Stachelhaus, T., Mootz, H.D., and Marahiel, M.A. (1999). The specificity-conferring code of adenylation domains in nonribosomal peptide synthetases. *Chem. Biol.* 6, 493–505. [https://doi.org/10.1016/S1074-5521\(99\)80082-9](https://doi.org/10.1016/S1074-5521(99)80082-9).
  31. Maruyama, C., Niikura, H., Takakuwa, M., Katano, H., and Hamano, Y. (2016). Colorimetric detection of the adenylation activity in nonribosomal peptide synthetases. *Methods Mol. Biol.* 1401, 77–84. [https://doi.org/10.1007/978-1-4939-3375-4\\_5](https://doi.org/10.1007/978-1-4939-3375-4_5).
  32. Wilson, D.J., and Aldrich, C.C. (2010). A continuous kinetic assay for adenylation enzyme activity and inhibition. *Anal. Biochem.* 404, 56–63. <https://doi.org/10.1016/j.ab.2010.04.033>.
  33. Duckworth, B.P., Wilson, D.J., and Aldrich, C.C. (2016). Measurement of nonribosomal peptide synthetase adenylation domain activity using a continuous hydroxylamine release assay. *Methods Mol. Biol.* 1401, 53–61. [https://doi.org/10.1007/978-1-4939-3375-4\\_3](https://doi.org/10.1007/978-1-4939-3375-4_3).
  34. Loweridge, E.J., Jones, C., Bull, M.J., Moody, S.C., Kahl, M.W., Khan, Z., Neilson, L., Tomeva, M., Adams, S.E., Wood, A.C., et al. (2017). Reclassification of the specialized metabolite producer *Pseudomonas mesoacidophila* ATCC 31433 as a member of the *Burkholderia cepacia* complex. *J. Bacteriol.* 199, e00125-17–e00117. <https://doi.org/10.1128/JB.00125-17>.
  35. Schweizer, H.P. (2001). Vectors to express foreign genes and techniques to monitor gene expression in *Pseudomonads*. *Curr. Opin. Biotechnol.* 12, 439–445. [https://doi.org/10.1016/s0958-1669\(00\)00242-1](https://doi.org/10.1016/s0958-1669(00)00242-1).
  36. Meisner, J., and Goldberg, J.B. (2016). The *Escherichia coli* rhaSR-PrhaBAD inducible promoter system allows tightly controlled gene expression over a wide range in *Pseudomonas aeruginosa*. *Appl. Environ. Microbiol.* 82, 6715–6727. <https://doi.org/10.1128/AEM.02041-16>.
  37. Hogan, A.M., Jeffers, K.R., Palacios, A., and Cardona, S.T. (2021). Improved dynamic range of a rhamnose-inducible promoter for gene expression in *Burkholderia* spp. *Appl. Environ. Microbiol.* 87, e0064721. <https://doi.org/10.1128/AEM.00647-21>.
  38. Hoffmann, L., Sague, M.-F., and Brüser, T. (2021). A tunable anthranilate-inducible gene expression system for *Pseudomonas* species. *Appl. Microbiol. Biotechnol.* 105, 247–258. <https://doi.org/10.1007/s00253-020-11034-8>.
  39. Retallack, D., Schneider, J.C., Chew, L., Ramseier, T., Allen, J., Patkar, A., Squires, C., Talbot, H., and Mitchell, J. (2006). *Pseudomonas fluorescens* – a robust expression platform for pharmaceutical protein production. *Microb. Cell Factories* 5, S28. <https://doi.org/10.1186/1475-2859-5-S1-S28>.
  40. Rackham, E.J., Gruschow, S., Ragab, A.E., Dickens, S., and Goss, R.J.M. (2010). Pacidamycin biosynthesis: identification and heterologous expression of the first uridyl peptide antibiotic gene cluster. *ChemBiochem* 11, 1700–1709. <https://doi.org/10.1002/cbic.201000200>.
  41. Fan, C., and Bobik, T.A. (2008). The PduX enzyme of *Salmonella enterica* is an L-threonine kinase used for coenzyme B12 synthesis. *J. Biol. Chem.* 283, 11322–11329. <https://doi.org/10.1074/jbc.M800287200>.
  42. Tavares, N.K., VanDrise, C.M., and Escalante-Semerena, J.C. (2018). *Rhodobacteriales* use a unique L-threonine kinase for the assembly of the nucleotide loop of coenzyme B12. *Mol. Microbiol.* 110, 239–261. <https://doi.org/10.1111/mmi.14100>.
  43. Andreassi, J.L., 2nd, and Leyh, T.S. (2004). Molecular functions of conserved aspects of the GHMP kinase family. *Biochemistry-U S A* 43, 14594–14601. <https://doi.org/10.1021/bi048963o>.
  44. Fan, C., Fromm, H.J., and Bobik, T.A. (2009). Kinetic and functional analysis of L-threonine kinase, the PduX enzyme of *Salmonella enterica*. *J. Biol. Chem.* 284, 20240–20248. <https://doi.org/10.1074/jbc.M109.027425>.
  45. Ma, M., Kutz-Naber, K.K., and Li, L. (2007). Methyl esterification assisted MALDI FTMS characterization of the orokinin neuropeptide family. *Anal. Chem.* 79, 673–681. <https://doi.org/10.1021/ac061536r>.
  46. Jumper, J., Evans, R., Pritzel, A., Green, T., Figurnov, M., Ronneberger, O., Tunyasuvunakool, K., Bates, R., Židek, A., Potapenko, A., et al. (2021). Highly accurate protein structure prediction with AlphaFold. *Nature* 596, 583–589. <https://doi.org/10.1038/s41586-021-03819-2>.
  47. Sampaleanu, L.M., Vallée, F., Thompson, G.D., and Howell, P.L. (2001). Three-dimensional structure of the argininosuccinate lyase frequently complementing allele Q286R. *Biochemistry-U S A* 40, 15570–15580. <https://doi.org/10.1021/bi011525m>.
  48. Afanasyev, O.I., Kuchuk, E., Usanov, D.L., and Chusov, D. (2019). Reductive amination in the synthesis of pharmaceuticals. *Chem. Rev.* 119, 11857–11911. <https://doi.org/10.1021/acs.chemrev.9b00383>.
  49. Setoi, H., Kayakiri, H., and Hashimoto, M. (1989). Diastereoselective synthesis of an  $\alpha$ ,  $\beta$ -diaminocarboxylic acid: an efficient synthesis of FR900490, an immunomodulating peptide isolated from a fungus. *Chem. Pharm. Bull.* 37, 1126–1127. <https://doi.org/10.1248/cpb.37.1126>.
  50. Ohfuné, Y., Tomita, M., and Nomoto, K. (1981). Total synthesis of 2'-deoxymugineic acid, the metal chelator excreted from wheat root. *J. Am. Chem. Soc.* 103, 2409–2410. <https://doi.org/10.1021/ja00399a046>.
  51. Ageno, G., Banfi, L., Giuseppe Guanti, G.C., Manghisi, E., Riva, R., and Rocca, V. (1995). Enantiospecific and diastereoselective synthesis of 4,4-disubstituted-3-amino-2-azetidinones, starting from D-serine. *Tetrahedron* 51, 8121–8134. [https://doi.org/10.1016/0040-4020\(95\)00427-A](https://doi.org/10.1016/0040-4020(95)00427-A).
  52. Passiniemi, M., and Koskinen, A.M. (2013). Garner's aldehyde as a versatile intermediate in the synthesis of enantiopure natural products. *Beilstein J. Org. Chem.* 9, 2641–2659. <https://doi.org/10.3762/bjoc.9.300>.
  53. Smith, M.W., and Snyder, S.A. (2013). A Concise total synthesis of (+)-scholarisine A empowered by a unique C–H arylation. *J. Am. Chem. Soc.* 135, 12964–12967. <https://doi.org/10.1021/ja406546k>.
  54. Mengel, A., and Reiser, O. (1999). Around and beyond Cram's rule. *Chem. Rev.* 99, 1191–1224. <https://doi.org/10.1021/cr980379w>.
  55. Spangenberg, T., Schoenfelder, A., Breit, B., and Mann, A. (2007). A new method for the synthesis of chiral beta-branched alpha-amino acids. *Org. Lett.* 9, 3881–3884. <https://doi.org/10.1021/ol071305m>.
  56. Lam, W.H., Rychli, K., and Bugg, T.D.H. (2008). Identification of a novel beta-replacement reaction in the biosynthesis of 2,3-diaminobutyric acid in peptidyl nucleoside mureidomycin. *Org. Biomol. Chem.* 6, 1912–1917. <https://doi.org/10.1039/b802585a>.
  57. Liu, N., Guan, H., Niu, G., Jiang, L., Li, Y., Zhang, J., Li, J., and Tan, H. (2021). Molecular mechanism of mureidomycin biosynthesis activated by introduction of an exogenous regulatory gene ssaA into *Streptomyces roseosporus*. *Sci. China Life Sci.* 64, 1949–1963. <https://doi.org/10.1007/s11427-020-1892-3>.
  58. Hickey, J.L., Sindhikara, D., Zultanski, S.L., and Schultz, D.M. (2023). Beyond 20 in the 21st century: prospects and challenges of non-canonical amino acids in peptide drug discovery. *ACS Med. Chem. Lett.* 14, 557–565. <https://doi.org/10.1021/acsmchemlett.3c00037>.
  59. Zou, H., Li, L., Zhang, T., Shi, M., Zhang, N., Huang, J., and Xian, M. (2018). Biosynthesis and biotechnological application of non-canonical amino acids: Complex and unclear. *Biotechnol. Adv.* 36, 1917–1927. <https://doi.org/10.1016/j.biotechadv.2018.07.008>.
  60. Taton, A., Lis, E., Adin, D.M., Dong, G., Cookson, S., Kay, S.A., Golden, S.S., and Golden, J.W. (2012). Gene transfer in *Leptolyngbya* sp. strain BL0902, a cyanobacterium suitable for production of biomass and bioproducts. *PLoS One* 7, e30901. <https://doi.org/10.1371/journal.pone.0030901>.
  61. Selvaraj, G., and Iyer, V.N. (1984). Transposon Tn5 specifies streptomycin resistance in *Rhizobium* spp. *J. Bacteriol.* 158, 580–589. <https://doi.org/10.1128/jb.158.2.580-589.1984>.
  62. Shaw, K.J., and Berg, C.M. (1979). *Escherichia coli* K-12 auxotrophs induced by insertion of the transposable element Tn5. *Genetics* 92, 741–747. <https://doi.org/10.1093/genetics/92.3.741>.
  63. Aoki, H., Sakai, H., Kohsaka, M., Konomi, T., and Hosoda, J. (1976). Nocardicin A, a new monocyclic beta-lactam antibiotic. I. Discovery, isolation and characterization. *J. Antibiot. (Tokyo)* 29, 492–500. <https://doi.org/10.7164/antibiotics.29.492>.
  64. Ishikawa, J., and Hotta, K. (1999). FramePlot: a new implementation of the frame analysis for predicting protein-coding regions in bacterial DNA with a high G + C content. *FEMS Microbiol. Lett.* 174, 251–253. <https://doi.org/10.1111/j.1574-6968.1999.tb13576.x>.
  65. Altschul, S.F., Gish, W., Miller, W., Myers, E.W., and Lipman, D.J. (1990). Basic local alignment search tool. *J. Mol. Biol.* 215, 403–410. [https://doi.org/10.1016/S0022-2836\(05\)80360-2](https://doi.org/10.1016/S0022-2836(05)80360-2).

STAR★METHODS

KEY RESOURCES TABLE

REAGENT or RESOURCE	SOURCE	IDENTIFIER
<b>Biological and chemical reagents</b>		
Restriction enzymes	New England Biolabs	neb.com
Modification enzymes	New England Biolabs	neb.com
HiFi DNA assembly master mix	New England Biolabs	E2621S
Phusion DNA polymerase	New England Biolabs	M0535
dNTP mix	Promega	U1515
[ $\alpha$ - <sup>32</sup> P]-dCTP	Perkin-Elmer	NEG007X250UC
Random DNA labeling system	Invitrogen	18187-013
Ni-NTA agarose	McLab	NINTA-100
Amicon 3K ultra spin columns	Sigma-Aldrich	UFC500396
General chemicals and buffers	Thermo Scientific	fisherscientific.com
Bacterial culture media	Boston Bioproduct	bostonbioproducts.com
Antibiotics	Gold Biotechnology	goldbio.com
L-Thr	Sigma-Aldrich	1721646
L-Ser	Sigma-Aldrich	1721404
OPT (9)	Sigma-Aldrich	1727078
OPS (6)	Sigma-Aldrich	1726826
L-Dap (3)	Matrix Scientific	#072732
D-Dap (11)	Chem-Impex	05645
(2S,3R)-Dab (4)	Lichstrahl, M.S.et al. <sup>18</sup>	N/A
(2S,3S)-Dab (10)	Boc Sciences	B18BS09181
L-2,4-Dab (12)	Alfa Aesar	L10093
Azide-Dab (13)	Lichstrahl, M.S.et al. <sup>18</sup>	N/A
Cl-Dab (14)	Lichstrahl, M.S.et al. <sup>18</sup>	N/A
Amino-Dab (15)	Lichstrahl, M.S.et al. <sup>18</sup>	N/A
Nitrocefin	Toku-E	N005
<b>Plasmids</b>		
pSCrhaB2plus	addgene	#164226
pSCrhaB2plus/Cm	This study	N/A
pSCrhaB2plus/sulK	This study	N/A
pACYC184	NEB	#E4152
pRK2013	Taton, A.et al. <sup>60</sup>	N/A
pJM101	addgene	#74740
pGS9	Selvaraj, and Iyer <sup>61</sup> , Shaw, and Berg <sup>62</sup>	N/A
pBluescript	Agilent Technologies	212205
pCR-Blunt	Life Technologies	K270040
pCR-Blunt/dabB	This study	N/A
pET29b	Millipore Sigma	69872
pET29b/dabB	This study	N/A
pET28b	Millipore Sigma	69865
pET28b/E264A3T3-3	This study	N/A

(Continued on next page)

**Continued**

REAGENT or RESOURCE	SOURCE	IDENTIFIER
pET28b/ <i>suIMA3T3</i>	This study	N/A
pUCP20-ANT2-MCS	Hoffmann, L. <sup>38</sup>	N/A
pUCP20-ANT2-MCS/ <i>Cm</i>	This study	N/A
pUCP20-ANT2-MCS/ <i>suIG</i>	This study	N/A
pUCP20-ANT2-MCS/ <i>suIGH</i>	This study	N/A
pUCP20-ANT2-MCS/ <i>dabABC</i>	This study	N/A
pUCP20-ANT2-MCS/ <i>dabBC</i>	This study	N/A
pUCP20-ANT2-MCS/ <i>dabC</i>	This study	N/A

**Bacterial strains**

<i>E. coli</i> PR47	Selvaraj, and Iyer <sup>61</sup> Shaw, and Berg <sup>62</sup>	N/A
<i>E. coli</i> DH5 $\alpha$	Thermo Fisher Scientific	18265017
<i>E. coli</i> Rosetta2 (DE3)	Sigma-Aldrich	70954
<i>E. coli</i> Rosetta2 (DE3) (pET29b/ <i>dabB</i> )	This study	N/A
<i>E. coli</i> Rosetta2 (DE3) (pET28b/ <i>suIMA3T3</i> )	This study	N/A
<i>E. coli</i> Rosetta2 (DE3) (pET28b/ <i>E264A3T3</i> )	This study	N/A
<i>E. coli</i> ESS	Aoki, H. <sup>63</sup>	N/A
<i>E. coli</i> HB101 (pRK2013)	ATCC	37159
<i>B. licheniformis</i> ATCC 14580	ATCC	14580
<i>P. acidophila</i> ATCC 31363	ATCC	31363
<i>P. acidophila</i> $\Delta$ <i>suIG</i>	This study	N/A
<i>P. acidophila</i> $\Delta$ <i>suIG/sulK::Tn5</i>	This study	N/A
$\Delta$ <i>suIG</i> (pUCP20-ANT2-MCS/ <i>Cm</i> )	This study	N/A
$\Delta$ <i>suIG</i> (pUCP20-ANT2-MCS/ <i>suIG</i> )	This study	N/A
$\Delta$ <i>suIG</i> (pUCP20-ANT2-MCS/ <i>suIGH</i> )	This study	N/A
$\Delta$ <i>suIG</i> (pUCP20-ANT2-MCS/ <i>dabABC</i> )	This study	N/A
$\Delta$ <i>suIG</i> (pUCP20-ANT2-MCS/ <i>dabBC</i> )	This study	N/A
$\Delta$ <i>suIG</i> (pUCP20-ANT2-MCS/ <i>dabC</i> )	This study	N/A
<i>B. thailandensis</i> E264	ATCC	700388
<i>B. thailandensis</i> $\Delta$ <i>scmR</i>	Guillouzer, L.S.et al. <sup>25</sup> et al. <sup>26</sup>	N/A
<i>E. coli</i> DH5 $\alpha$ (pSCrhaB2plus/ <i>Cm</i> )	This study	N/A
<i>E. coli</i> DH5 $\alpha$ (pSCrhaB2plus/ <i>suIK</i> )	This study	N/A

**Software and algorithms**

antiSmash	Blin, K. <sup>24</sup>	<a href="http://antismash.secondarymetabolites.org">antismash.secondarymetabolites.org</a>
FramePlot 4.0beta	Ishikawa, J., and Hotta, K. <sup>64</sup>	<a href="http://nocardia.nih.gov/jp/fp4/">nocardia.nih.gov/jp/fp4/</a>
BLAST	Altschul, S.F.et al. <sup>65</sup>	<a href="http://blast.ncbi.nlm.nih.gov/blast.cgi">blast.ncbi.nlm.nih.gov/blast.cgi</a>
AlphaFold	Jumper, J.et al. <sup>46</sup>	<a href="http://alphafold.ebi.ac.uk">alphafold.ebi.ac.uk</a>
UPLC-HRMS data analysis	Waters	MassLynx

**Other**

UPLC-HRMS	Waters	Acquity/Xevo-G2
PCR cyler	Bio-Rad	T100 Thermal Cycler
Electroporator	Life-Technologies	Cell-Porator™
UV-VIS spectrophotometer	Varian	Cary 50
NMR	Bruker	UltraShield 300 or 400 MHz Avance

(Continued on next page)

**Continued**

REAGENT or RESOURCE	SOURCE	IDENTIFIER
CombiFlash	Teledyne ISCO	EZ Prep
Supelclean™ ENVI-Carb™ SPE Tube	Supelco Analytical	57092

**Primers**

Primers	Sequences	Targets
dabB-F dabB-R	5'-GGGCATATGACACA CGACTGCATCGAACA-3' 5'-GGGGGATCCCGCGTCTGA GCGCGACGAGCTCCTG-3'	pET29b/ <i>dabB</i>
Cm-pSCrha-F Cm-pSCrha-R	5'-TGAAATTCAGCAGGATCACA-3' 5'-TGCATGCCTGCAGTTCGACTTT ACGCCCGCCCTGCCA-3'	pSCrhaB2plus/ <i>Cm</i>
sulK-28b-F sulK-28b-R	5'-GGGCATATGACACGAGATC GGCAATGGCA-3' 5'-GGGAAGCTTTTAGCAGCCG GATCTCAGTGGTGGTGG-3'	pET28b/ <i>sulK</i>
E264A3T3-3-F E264A3T3-R	5'-GGGCATATGGTGCTGCGC CAGGGTGAGCTGCGG-3' 5'-GGGAAGCTTCAGATGCG CGGCGAGCGCCTC-3'	pET28b/E264A3T3
pUCP20-Cm-F pUCP20-Cm-R	5'-GGGCATATGGAGAAA AAAATCACTGG-3' 5'-GGGAAGCTTTTACGCC CCGCCCTGCCAC-3'	pUCP20-ANT2-MCS/ <i>Cm</i>
pUCP20-sulG-F pUCP20-sulG-R	5'-AACTAGTAGGAGATATAC ATATGAAATTCAACTCAATCGA AC-3' 5'-TAAAACGACGGCCAGTGCCAC TAGACATACGCCAGAGTC-3'	pUCP20-ANT2-MCS/ <i>sulG</i>
pUCP20-sulGH-F pUCP20-sulGH-R	5'-AACTAGTAGGAGATATACATAT GAAATTCAACTCAATCGA AC-3' 5'-TAAAACGACGGCCAGTGCCAC TACATGGTCCACCGTTC-3'	pUCP20-ANT2-MCS/ <i>sulGH</i>
pUCP20-dabABC-F pUCP20-dabABC-R	5'-AACTAGTAGGAGATATACATA TGAGCATCATCGAGAACAAC GAAGACC-3' 5'-TAAAACGACGGCCAGTGCCAT CAGTCGCCCGCCAGCTG-3'	pUCP20-ANT2-MCS/ <i>dabABC</i>
pUCP20-dabBC-F pUCP20-dabBC-R	5'-AACTAGTAGGAGATATACATATGA CACACGACTGCAT CGAAC-3' 5'-TAAAACGACGGCCAGTGCCATC AGTCGCCCGCCAGCTG-3'	pUCP20-ANT2-MCS/ <i>dabBC</i>
pUCP20-dabC-F pUCP20-dabC-R	5'-AACTAGTAGGAGATATACATATGAC GGGTATCTTTGTCTTC ATCGAGAGC-3' 5'-TAAAACGACGGCCAGTGCCATCAG TCGCCCGCCAGCTG-3'	pUCP20-ANT2-MCS/ <i>dabC</i>

**RESOURCE AVAILABILITY**

**Lead contact**

Further information and requests for resources and reagents should be directed to and will be fulfilled by the lead contact: Prof. Craig A. Townsend ([ctownsend@jhu.edu](mailto:ctownsend@jhu.edu)).

### Materials availability

This study did not generate new unique reagents.

### Data and code availability

- DabA, DabB, and DabC data have been deposited at GenBank and are publicly available as of the date of publication, under the accession number GenBank: BK065153 at NCBI's GenBank database.
- This paper does not report original codes.
- Any additional information required to reanalyze the data reported in this paper is available from the [lead contact](#) upon request.

## EXPERIMENTAL MODEL AND STUDY PARTICIPANT DETAILS

This research does not involve models or human/animal participants.

### METHOD DETAILS

#### Construction of recombinant plasmids

All recombinant plasmids were confirmed by DNA sequence analysis (The Synthesis & Sequencing Facility at The Johns Hopkins University).

Construction of pSCrhaB2plus/Cm: The chloramphenicol-resistant gene was amplified from plasmid pACYC184 using primers Cm-pSCrha-F and Cm-pSCrha-R. The PCR product was assembled with *NdeI/XbaI*-digested pSCrhaB2plus using NEBuilder(R) HiFi DNA Assembly Master Mix (New England Biolabs) to give recombinant pSCrhaB2plus/Cm.

Construction of pSCrhaB2plus/sulK: *sulK* was amplified from genomic DNA of the WT *P. acidophila* using primers sulK-28b-F and sulK-28b-R. The PCR product was digested with *NdeI* and *HindIII* and ligated to *NdeI/HindIII*-digested pET28b to give recombinant plasmid pET28b/sulK. pET28b/sulK was digested with *BlnI*, blunt-ended with Klenow DNA polymerase, and digested with *NdeI*. The resulting *sulK* fragment was ligated into *NdeI/XmnI*-digested pSCrhaB2plu to generate pSCrhaB2plus/sulK.

Construction of pET29b/dabB: *dabB* was amplified from the genome of *B. thailandensis* E264 using primers dabB-F and dabB-R. The PCR product was ligated into plasmid pCR-Blunt and gave pCR-Blunt/dabB. *dabB* was excised with *NdeI* and *BamHI* and ligated into *NdeI/BamHI*-digested pET29b to give expression vector pET29b/dabB.

Construction of pET28b/E264A3T3-3: The fragment encoding A3T3 and upstream 16-a.a. linker region between the epimerization and adenylation domains was amplified using primers E264A3T3-3-F and E264A3T3-3-R. The PCR product was digested with *NdeI/HindIII* and ligated into pET28b digested with the same enzymes to generate expression vector pET28b/E264A3T3-3.

Construction of pUCP20-ANT2-MCS/Cm: The chloramphenicol-resistant gene was amplified from plasmid pACYC184 using primers pUCP20-Cm-F and pUCP20-Cm-R. The PCR product was digested with *NdeI/HindIII* and ligated into *NdeI/HindIII*-digested pUCP20-ANT2-MCS to give the expression vector pUCP20-ANT2-MCS/Cm.

Construction of pUCP20-ANT2-MCS-derived expression vectors: The biosynthetic genes *sulG*, *sulGH*, *dabABC*, *dabBC*, and *dabC* were amplified by PCR using primers listed in [key resources table](#) from the *P. acidophila* and *B. thailandensis* genomes. The PCR products were assembled with *NdeI/HindIII*-digested pUCP20-ANT2-MCS using NEBuilder(R) HiFi DNA Assembly Master Mix (New England Biolabs) to give recombinants pUCP20-ANT2-MCS/sulG, pUCP20-ANT2-MCS/sulGH, pUCP20-ANT2-MCS/dabABC, pUCP20-ANT2-MCS/dabBC, and pUCP20-ANT2-MCS/dabC, respectively.

#### Generation and identification of *sulK* transposon mutant in *P. acidophila*

A mutant library consisting of approximately 5,000 potentially independent Tn5 transposon insertional mutants of *P. acidophila*  $\Delta$ *sulG* was constructed by biparental mating between *P. acidophila*  $\Delta$ *sulG* and *E. coli*. A single colony of *P. acidophila*  $\Delta$ *sulG* or *E. coli* PR47 was inoculated into 15 mL of sulfazecin seed medium or LB (Km) and cultures were grown at 30°C or 37°C for approximately 15 h to OD<sub>600</sub> = 0.8 and 1.6, respectively, and 1 mL of PR47 and 2 mL of *P. acidophila*  $\Delta$ *sulG* was harvested and washed with LB medium. Each cell type was resuspended in 0.5 mL LB medium, mixed in a 1:1 (donor/ recipient) ratio, and 200  $\mu$ L of the mixed cells was plated on each King's B agar plate (g/L: peptone 20; K<sub>2</sub>HPO<sub>4</sub> 1.5; MgSO<sub>4</sub> 1.5; glycerol 10; agar 20), followed by incubation at 30°C for 20 h. The resulting mated cells were harvested and resuspended in 10 mL of 10 mM NaPPi buffer (pH 7.0). 10 X serial dilutions were made from the cell suspension and 100  $\mu$ L of each dilution was spread on YM agar (g/L: K<sub>2</sub>HPO<sub>4</sub> 0.5; MgSO<sub>4</sub> 0.2; NaCl 0.1; yeast extract 1.0; mannitol 10) containing 100  $\mu$ g/mL carbenicillin (Car), 50  $\mu$ g/mL Gentamicin (Gm) and 50  $\mu$ g/mL Km. Car<sup>R</sup>/Km<sup>R</sup>/Gm<sup>R</sup> exconjugants were obtained after growing at 30°C for 4-6 days.

To identify the *sulK* mutant, genomic DNA was digested with several restriction enzymes including *BamHI*, *BstBI*, *DrallI*, *EcoRI*, *EcoRV*, *KpnI*. The digested genomic DNAs were hybridized with an [ $\alpha$ -<sup>32</sup>P]-dCTP-labeled kanamycin-resistant fragment isolated from Tn-5 by digestion of plasmid pGS9 with *HindIII*. The 5-kb positive fragment from the *BamHI*-digested genome was cloned into pBluescript to give plasmid pBluescript/Bam5.0. The plasmid was subjected to DNA sequence analysis to identify the location of Tn-5 insertion.

#### Protein expression and purification

Expression vectors pET29b/dab, pET28b/sulMA3T3 and pET28b/E264A3T3-3 were transformed into *E. coli* Rosetta2 (DE3) by electroporation and selected on LB (Cm, Km) plates, respectively. A single colony was inoculated into LB (Cm, Km) seed medium and seed cultures were

grown at 37°C for 12-15 h before inoculating expression medium (LB+2% glycerol, or TB, Cm, Km) in either 2.8-L non-baffled flasks or in 5-L bioreactor. Cultures were grown at 37°C to  $OD_{600} = 0.6 - 0.7$  and chilled immediately in an ice-water bath for 30 min and followed by induction with 0.5 or 1 mM IPTG. Expression was carried out at 20°C for 24 h. His-tagged proteins were purified with standard Ni-NTA affinity chromatography as described by the manufacturer (Gold Biotechnology, St. Louis, MO).

### Transformation, gene expression and fermentation of *B. thailandensis*

*B. thailandensis* E264 and  $\Delta scmR$  were grown on LB agar. The LB seed medium was inoculated from a freshly grown LB plates and grew at 37°C for 24 h before being transferred into sulfazecin fermentation medium, Medium 2 (g/L, glycerol 10, glucose 1,  $Na_2S_2O_3$  1, peptone 5, meat extract 5, NaCl 5, L-Glu 1, L-Ala 1, L-Thr 1, Cystine 0.2, L-Met 0.2,  $ZnSO_4 \cdot 7H_2O$  0.001, pH 7.0), or Medium 3 (g/L tryptone 5, peptone 5, meat extract 5, glucose 10, fructose 10,  $Na_2S_2O_3$  1, L-Thr 1, pH 7.0) at 1/20 ratio. Fermentation was carried out at 37°C for 96 h with rotation at 250 rpm.

pSCrhaB2plus expression vectors in *E. coli* DH5 $\alpha$  were delivered into *B. thailandensis*  $\Delta scmR$  through a triparental conjugation with HB101 (pKR2013) helper strain. 5 mL of each strain was grown for 15 h at 37°C with proper antibiotic selection. 150  $\mu$ L of each culture was mixed and cells were collected by centrifugation at 13K rpm for 2 min. After 2X washing with 2 mL LB medium, cells were resuspended in 300  $\mu$ L LB and spread on a nylon membrane sitting on LB agar plate. The plate was incubated at 37°C for 12 h and cells were scraped and washed 1X with LB medium before being resuspended in 300  $\mu$ L LB. 100  $\mu$ L cells were plated on LB containing 150  $\mu$ g/mL trimethoprim (TMP), 60  $\mu$ g/mL gentamicin (Gm) and incubated at 37°C for 2-3 d to select exconjugants. To test the genetic stability of exconjugants, plasmids were purified and ~0.1-0.5  $\mu$ g was used to transform *E. coli* DH5 $\alpha$ . Plasmids purified from DH5 $\alpha$  transformants were subjected to analysis by restriction digestions.

To test the  $P_{rhaBAD}$  strength using a reporter gene in *B. thailandensis*  $\Delta scmR$  (pSCrhaB2plus/Cm), a 5-mL culture containing 150  $\mu$ g/mL TMP, 10  $\mu$ g/mL Gm and 0.1% rhamnose was grown at 37°C for 24 h with 250 rpm rotation. 10  $\mu$ L of culture was spotted on LB agar containing 150  $\mu$ g/mL TMP and 70  $\mu$ g/mL chloramphenicol (Cm) and incubated at 37 °C for 2–3 d. *B. thailandensis*  $\Delta scmR$  (pSCrhaB2plus) was used as negative control. A similar protocol was used for expression of *sulK* in *B. thailandensis*  $\Delta scmR$  (pSCrhaB2plus/*sulK*) but 0.2% rhamnose was used for induction. Supernatants of induced and uninduced  $\Delta scmR$  (pSCrhaB2plus/*sulK*) were withdrawn every 24 h during fermentation and tested for production of MM42842 using the nitrocefin assay.

### Transformation, gene expression and fermentation of *P. acidophila*

*P. acidophila* and its transformants were grown on sulfazecin seed agar (g/L: glucose 10, peptone 5, meat extract 5, NaCl 5, agar 20, pH 7.0) at 30°C. 50  $\mu$ g/mL kanamycin (Km) was added if cells harboring pUCP20-ANT2-MCS derived plasmids. For growing in liquid medium, 50-mL sulfazecin seed medium was inoculated from a fresh plate and grown at 28°C for 60-72 h with 250 rpm rotation. 50  $\mu$ g/mL Km was added if cells harboring pUCP20-ANT2-MCS derived plasmids. 2.5 mL seed culture was transferred to 50 mL sulfazecin fermentation medium (g/L: glycerol 30, glucose 1,  $Na_2S_2O_3$  1, peptone 5, meat extract 5, NaCl 5, cystine 0.2, pH 6.3). Fermentation was carried out at the same conditions as the seed culturing for 120 h. For chemical feeding with L-Dap (3) or (2S,3R)-Dab (4), the amino acid was added to 24-h fermentation cultures. The final concentration of each amino acid was 2 mM or 3 mM.

To transform the WT or its mutants, 1-2  $\mu$ g of plasmid was mixed with 30  $\mu$ L electroporation-competent cells. Electroporation was carried out at 1.9-2.0 kv using a BRL Cell-Porator. The transformed cells were immediately mixed with 2 mL of sulfazecin seed medium and incubated at 28°C for 8 h with rotation (250 rpm). Cells were collected by centrifugation at 17000 x g for 3 min and resuspended in 200  $\mu$ L sulfazecin seed medium. 100  $\mu$ L was plated on each sulfazecin seed agar plate containing 50  $\mu$ g/mL Km. The plates were incubated at 30°C for 5 d until the resistant colonies appeared.

To induce gene expression in pUCP20-ANT2-MCS constructs for genetic complementation, the seed culture of transformants was transferred to 50 mL fermentation medium at a 1:20 ratio. To test the  $P_{antA}$  strength using a reporter, expression of the chloramphenicol resistance gene was induced with 0, 0.3, 0.4, and 0.5 mM anthranilate at the beginning of fermentation, respectively. After 2 d, 100  $\mu$ L of each culture was plated on sulfazecin seed agar containing 50  $\mu$ g/mL Km and 80  $\mu$ g/mL Cm. Plates were incubated at 30°C for 3-4 d.

For genetic complementation in  $\Delta sulG$  with pUCU20-ANT2-MCS expression constructs, anthranilate was added to a concentration of 0.5 mM at the beginning of fermentation. More anthranilate was added after 24 h of fermentation to the final concentration of 1.0 mM. Production of monobactams was examined at 72 or 96 h of fermentation. For administration of ACPAA (17) to  $\Delta sulG$  (pUCP20-ANT2-MCS/*dabC*), the compound was dissolved in 25 mM tris(hydroxymethyl)aminomethane hydrochloride (Tris-HCl, pH7.5), 50 mM NaCl, 5% glycerol and the pH was adjusted to 6.5 using 1 M NaOH. ACPAA (17) was added to the fermentation culture 24 h after expression of *dabC* was induced.

### Detection of monobactam activities in *P. acidophila*

Fermentation broth (2 mL) was withdrawn and centrifuged for 3 min at 16000 x g. The antibacterial activity was assayed by using 250  $\mu$ L supernatant against *E. coli* ESS seeded (0.4%) in nutrient agar. To analyze  $\beta$ -lactam products from fermentation, 250  $\mu$ L supernatant was assayed on *B. licheniformis* ATCC 14580 mixed with 100 mL BA2 agar (g/L: BBL seed agar 30.5, NaCl 5). The plate was incubated for 5 h at 37°C and induction of  $\beta$ -lactamase was visualized by overlaying with 1.5 mL of 40  $\mu$ g/mL nitrocefin solution in phosphate buffer (pH 7.0).

A Supelclean™ ENVI-Carb™ SPE Tube (250 mg bed wt.) was conditioned with 2 mL of water and 2 mL of 50% acetonitrile, then equilibrated with 3 mL of water by gravity flow. A 500  $\mu$ L supernatant was loaded on to the column, then washed with 2.5 mL of water by gravity flow. Products were eluted in 400  $\mu$ L fractions of 50% acetonitrile by gravity flow, which were collected separately. Each elution fraction was directly

analyzed (negative ion mode) by UPLC-HRMS as follows: ES- [binary gradient: water (solvent A), acetonitrile (solvent B), 0.3 mL/min]: 0-1 min isocratic 20% A; 1-7.5 min gradient 20% to 100% A; 7.5-8.4 min isocratic 100% A; 8.4-8.5 min gradient 100% to 20% A; 8.5-10 min isocratic 20% A. Waters ACQUITY UPLC BEH Amide Column, 130 Å, 1.7 μm, 2.1 mm × 100 mm. Monobactam products were detected between fractions two and four.

### E264 and SulM A-domain pyrophosphate assay

A-domain activity was measured through colorimetric detection of released pyrophosphate using a modified *in vitro* assay. Each reaction was performed on a 100 μL scale containing 50 mM Tris-HCl, pH 8.0, 5 mM magnesium chloride (MgCl<sub>2</sub>), 5 mM adenosine 5'-triphosphate (ATP), 5 mM amino acid substrate, 40 mM hydroxylamine and purified A3T3 to a final concentration of 130 μg/mL (approx. 1.8 μM). Reactions were initiated by addition of enzyme and incubated for 70 min at 30°C. 1 mL Mo(VI) solution (20 mM sodium molybdate (NaMoO<sub>4</sub>) in 0.6 M hydrochloric acid and 60% acetonitrile) was added, vortexed briefly, and samples were incubated for 5 min at room temperature. 20 μL of bis(tri-phenylphosphoranylidene)ammonium chloride (BTPPACl, 50 mM in acetonitrile) was added, vortexed briefly, and samples were incubated for 5 min at room temperature. The mixture was then centrifuged for 20 min at 16,000 × g. After removal of the supernatant, the pellet was dissolved in 200 μL of acetonitrile. 20 μL ascorbic acid (0.5 M in 2 M hydrochloric acid and 60% acetonitrile) was added and the mixture was incubated at room temperature for 10 min. 200 μL acetonitrile was added and the absorbance at 620 nm was measured using a Varian Cary 50 UV-Vis spectrophotometer. Each amino acid substrate was blanked against an identical sample with no added enzyme.

### Biochemical analysis of DabB

UV-vis spectral analyses of the DabB reactions were collected on a Varian Cary 50 UV-Visible spectrophotometer. The DabB-PLP spectra were measured at a concentration of 0.8 mg/mL in 50 mM 2-[4-(2-hydroxyethyl)piperazin-1-yl]ethanesulfonic acid (HEPES, pH 7.5, 100 mM NaCl, 10% glycerol at room temperature. To measure the formation of the DabB aminoacylate aldimine complex, OPT (9) or OPS (6) was mixed with DabB at final concentrations of 0.1 mM and 0.8 mg/mL and spectra were recorded immediately. To identify the amine donors and return of the resting state of DabB, L-Asp or L-Glu was added to DabB-OPT or DabB-OPS to a final concentration of 2 mM and 5 mM, respectively. The mixture was incubated at room temperature for 5 min before the spectra were recorded.

The *in vitro* assays for the formation of ACPAA by DabB were performed in 1-mL reactions containing the following components: 2 mg/mL purified DabB, 2 mg/mL OPT (9), and 6 mg/mL L-Asp in 25 mM Tris-HCl, pH 7.5, 50 mM NaCl, 10% glycerol. The negative control reaction had the same components but DabB. The reaction mixture was incubated at 30°C for 1 h and DabB was removed using Sigma-Aldrich Amicon 3K spin filters by centrifugation at 4000 × g for 30 min. The flow-through was lyophilized and resuspended in freshly made methanolic HCl. Esterification was performed at 37°C for 10 h and concentrated to dryness by rotary evaporation. The esterified ACPAA (17) was resuspended in 50% acetonitrile containing 0.1% formic acid for analysis by UPLC-HRMS.

The *in vitro* assays for the formation of ACEAA (16) by DabB were performed in 1-mL reactions containing the following components: 3 mg/mL purified DabB, 2 mg/mL OPS (9), and 6 mg/mL L-Asp in 25 mM Tris-HCl, pH 7.5, 50 mM NaCl, 10% glycerol. The negative control reaction had the same components but DabB. The reaction mixture was incubated at 30°C for 1 h and DabB was removed using Sigma-Aldrich Amicon 3K spin filters by centrifugation at 4000 × g for 30 min. The flow-through was lyophilized and resuspended in freshly made methanolic HCl. Esterification was performed at 37°C for 10 h and concentrated to dryness by rotary evaporation. The esterified ACEAA (16) was resuspended in 50% acetonitrile containing 0.1% formic acid for analysis by UPLC-HRMS.

### Synthesis of ACPAA

*tert*-Butyl (R)-4-(methoxy(methyl)carbamoyl)-2,2-dimethyloxazolidine-3-carboxylate (19)

Compound 19 (Figure 6) was prepared according to a known procedure. Spectral data were consistent with literature values.

*tert*-Butyl (R)-4-acetyl-2,2-dimethyloxazolidine-3-carboxylate (20)

Compound 19 (Figure 6) (2.88 g, 10.0 mmol) was placed in a dry flask under Argon and dissolved in 30 mL of anhydrous tetrahydrofuran. The solution was cooled to -78°C and methylmagnesium bromide (6.66 mL, 20.0 mmol, 3.0 M in diethyl ether) was added dropwise. The reaction was stirred at this temperature 30 min, then allowed to warm to room temperature and stirred until complete consumption of the starting material was observed by thin layer chromatography. A saturated aqueous solution of ammonium chloride (30 mL) was added carefully and stirred at room temperature for 15 min. The mixture was extracted 3 × 30 mL of ethyl acetate, and the combined organics were washed with 30 mL of saturated brine, dried over anhydrous sodium sulfate and concentrated. Purification by flash chromatography (8/2 hexanes/ethyl acetate) yielded 20 (Figure 6) as a colorless oil (2.17 g, 90%). Spectral data were consistent with those observed in the literature.

Dibenzyl (1-((S)-3-(*tert*-butoxycarbonyl)-2,2-dimethyloxazolidin-4-yl)ethyl)-L-aspartate (21)

Compound 20 (1.03 g, 4.25 mmol) and dibenzyl-L-aspartate *p*-toluenesulfonate (2.48 g, 5.11 mmol) were dissolved in 20 mL of methanol. Sodium cyanoborohydride (402 mg, 6.38 mmol) was added and the reaction was stirred at room temperature for 18 h. A saturated aqueous solution of ammonium chloride (30 mL) was carefully added, and the mixture was stirred for 15 min before the methanol was removed by rotary evaporation. The aqueous phase was extracted 3 × 30 mL of ethyl acetate and the combined organics were washed with 30 mL of

saturated brine, dried over anhydrous sodium sulfate and concentrated. Purification by flash chromatography (9/1 8/2 hexanes/ethyl acetate) afforded **21** (1.75 g, 76%) as a ~ 2:1 mixture of diastereomers.

$^1\text{H NMR}$  (400 MHz;  $\text{CDCl}_3$ ):  $\delta$  7.42-7.30 (m, 10H), 5.22-5.03 (m, 4H), 4.07-3.66 (m, 4H), 3.24-3.01 (m, 1H), 2.86-2.60 (m, 2H), 1.64-1.40 (m, 15H), 1.02 (d,  $J = 6.7$  Hz, 0.8H), 0.97 (d,  $J = 6.5$  Hz, 2.2H);  $^{13}\text{C NMR}$  (100 MHz;  $\text{CDCl}_3$ ):  $\delta$  173.8, 170.7, 166.6, 153.3, 152.3, 135.8, 135.7, 129.0, 128.9, 128.7, 128.5, 128.4, 94.6, 94.1, 86.3, 80.2, 68.5, 67.1, 66.7, 63.9, 63.3, 62.2, 60.6, 60.2, 57.1, 55.9, 52.8, 52.7, 38.9, 28.6, 28.0, 19.2; **HRMS** (ESI)  $m/z$ :  $[\text{M}+\text{H}]^+$  calculated 541.2908, found 541.2916. [Figures S9A](#) and [S9B](#).

#### Dibenzyl ((2*S*,3*S*)-3-((*tert*-butoxycarbonyl)amino)-4-hydroxybutan-2-yl)-l-aspartate and dibenzyl ((2*S*,3*R*)-3-((*tert*-butoxycarbonyl)amino)-4-hydroxybutan-2-yl)-l-aspartate (**22a** and **22b**)

Acetyl chloride (6 mL) was added dropwise to 36 mL of methanol at 0°C and stirred for 15 min. Compound **21** ([Figure 6](#)) (1.75 g, 3.24 mmol) was dissolved in 15 mL of methanol and added to the above solution at 0°C, and the reaction was stirred at this temperature for 3 h. The solvent was removed by rotary evaporation and concentrated under high vacuum. The residue was re-dissolved in 50 mL of dichloromethane and cooled to 0°C. Di-*tert*-butyl dicarbonate (1.41 g, 6.48 mmol) and *N,N*-diisopropylethylamine (2.82 mL, 16.2 mmol) were added and the reaction was allowed to warm to room temperature and stirred for 18 h. A saturated aqueous solution of ammonium chloride (50 mL) was added and the layers were separated. The aqueous phase was extracted 2  $\times$  30 mL of dichloromethane and the combined organics were dried over anhydrous sodium sulfate and concentrated. Purification by flash chromatography (55/45 50/50 hexanes/ethyl acetate) afforded **22a** (first eluting) and **22b** (second eluting) (534 mg, 33%), of which 50 mg were a 10:1 mixture of **22a/22b**, 86 mg were a 1:1 mixture of **22a/22b**, 112 mg were a 1:8 mixture of **22a/22b** and 286 mg were pure **22b**. A fraction of each diastereomer could be cleanly isolated to obtain characterization.

##### **22a** ([Figure 6](#)).

$^1\text{H NMR}$  (400 MHz;  $\text{CDCl}_3$ ):  $\delta$  7.36-7.26 (m, 10H), 5.53 (d,  $J = 6.4$  Hz), 5.15-5.05 (m, 4H), 3.88 (dd,  $J = 11.5, 3.4$  Hz, 1H), 3.81 (dd,  $J = 8.3, 4.5$  Hz, 1H), 3.53 (dd,  $J = 11.5, 3.4$  Hz, 1H), 3.44-3.34 (m, 1H), 3.00-2.89 (m, 1H), 2.68 (ABX,  $J_{AB} = 16.0$ ,  $J_{AX} = 8.3$ ,  $J_{BX} = 4.5$  Hz, 2H), 1.41 (s, 9H), 1.08 (d,  $J = 6.7$  Hz);  $^{13}\text{C NMR}$  (100 MHz;  $\text{CDCl}_3$ ):  $\delta$  173.5, 170.8, 156.6, 135.5, 135.3, 128.8, 128.8, 128.7, 128.7, 128.6, 79.7, 67.6, 67.2, 63.0, 57.5, 55.4, 53.8, 38.5, 28.6, 18.1 **HRMS** (ESI)  $m/z$ :  $[\text{M}+\text{H}]^+$  calculated 501.2595, found 501.2602. [Figures S9C](#) and [S9D](#).

##### **22b** ([Figure 6](#))

$^1\text{H NMR}$  (400 MHz;  $\text{CDCl}_3$ ):  $\delta$  7.37-7.26 (m, 10H), 5.23-5.15 (m, 1H), 5.15-5.03 (m, 4H), 3.77 (dd,  $J = 7.9, 4.7$  Hz, 1H), 3.73-3.60 (m, 2H), 3.53-3.43 (m, 1H), 2.96-2.85 (m, 1H), 2.71 (ABX,  $J_{AB} = 16.0$ ,  $J_{AX} = 8.0$ ,  $J_{BX} = 4.7$  Hz, 2H), 1.43 (s, 9H), 1.02 (d,  $J = 6.4$  Hz);  $^{13}\text{C NMR}$  (100 MHz;  $\text{CDCl}_3$ ):  $\delta$  173.6, 170.6, 156.7, 135.5, 135.4, 128.8, 128.8, 128.8, 128.7, 128.7, 128.6, 79.7, 67.4, 67.0, 65.3, 55.5, 55.3, 53.9, 38.4, 28.6, 17.5; **HRMS** (ESI)  $m/z$ :  $[\text{M}+\text{H}]^+$  calculated 501.2595, found 501.2602. [Figures S9E](#) and [S9F](#).

#### (2*S*,3*R*)-3-(((*S*)-1,4-Bis(benzyloxy)-1,4-dioxobutan-2-yl)amino)-2-((*tert*-butoxycarbonyl)amino)butanoic acid (**23**).

The procedure of Spangenberg et al. was used with minor modifications.<sup>55</sup>

A stock solution of Periodic acid/Chromium (VI) oxide was prepared by dissolving periodic acid (2.0 g, 8.77 mmol) and chromium (VI) oxide (4.0 mg, 0.04 mmol) in 19.8 mL of acetonitrile and 0.20 mL of water.

Compound **22b** ([Figure 6](#)) (286 mg, 0.572 mmol) was dissolved in 5 mL of acetonitrile and cooled to 0°C, then 4.0 mL of the stock solution of periodic acid (1.66 mmol)/chromium (IV) oxide (0.008 mmol) was added dropwise. The reaction was stirred at this temperature for 1 h, then an additional 1.0 mL of the stock solution (0.44 mmol of periodic acid, 0.002 mmol chromium (IV) oxide) was added. After 30 min, the reaction was quenched by the addition of 20 mL of 100 mM potassium phosphate buffer pH 5.8. The mixture was extracted 3  $\times$  20 mL of ethyl acetate, washed with 20 mL of saturated brine, dried over anhydrous sodium sulfate and concentrated. Purification by flash chromatography (1/1 hexanes/ethyl acetate 1% acetic acid) yielded **23** ([Figure 6](#)) (197 mg, 67%) as a colorless oil.

$^1\text{H NMR}$  (400 MHz;  $\text{CDCl}_3$ ):  $\delta$  7.38-7.26 (m, 10H), 5.54 (d, 4.8 Hz, 1H), 5.14 (ABq,  $J = 12.1$  Hz, 2H), 5.06 (s, 2H), 4.17 (t,  $J = 4.4$  Hz, 1H), 3.93 (t,  $J = 5.0$  Hz, 1H), 3.45-3.36 (m, 1H), 2.92 (d,  $J = 5.0$  Hz, 2H), 1.41 (s, 9H), 1.02 (d,  $J = 6.6$  Hz);  $^{13}\text{C NMR}$  (100 MHz;  $\text{CDCl}_3$ ):  $\delta$  171.6, 171.4, 170.5, 155.6, 135.3, 135.0, 128.8, 128.7, 128.7, 80.3, 68.0, 67.2, 55.5, 54.6, 51.9, 35.7, 28.4, 14.4; **HRMS** (ESI)  $m/z$ :  $[\text{M}+\text{H}]^+$  calculated 515.2388, found 515.2393. [Figures S9G](#) and [S9H](#).

#### (1*S*,2*R*)-1-Amino-1-carboxypropan-2-yl)-l-aspartic acid (ACPAA) dihydrochloride. (**17**)

Compound **23** ([Figure 6](#)) (35 mg, 0.068 mmol) was dissolved in 5 mL of methanol and 10% palladium on carbon (7 mg) was added. The reaction was placed in a pressure tube and shaken on a Parr apparatus under 40 psi of hydrogen gas for 18 h at room temperature. The solution was filtered over Celite and rinsed with methanol, then concentrated to obtain a white solid. The residue was dissolved in 4 mL of 98% formic acid and stirred at room temperature for 6 h. The reaction mixture was concentrated, then 3 mL of a 100 mM aqueous solution of hydrochloric acid was added and the solution was stirred at room temperature for 5 min. The water was removed under reduced pressure and this procedure was repeated three times. After the final repetition, the residue was dissolved in 3 mL of water, transferred to a tared vial, frozen and lyophilized to dryness to afford **ACPAA** ([Figure 6](#)) (20 mg, 96%) as an off-white, hygroscopic solid.

$^1\text{H NMR}$  (400 MHz;  $\text{D}_2\text{O}$ ):  $\delta$  4.54 – 4.51 (dd,  $J = 8, 3.9$  Hz, 1H), 4.45 (d,  $J = 3.2$ , 1H), 4.00 – 3.94 (m, 1H), 3.24 – 3.18 (dd,  $J = 18.4, 3.9$  Hz, 1H), 3.12 – 3.05 (dd,  $J = 18.4, 7.8$  Hz, 1H), 1.42 (d,  $J = 6.7$  Hz, 1H);  $^{13}\text{C NMR}$  (100 MHz;  $\text{D}_2\text{O}$ ):  $\delta$  173.3, 170.2, 169.0, 55.5, 53.2, 53.0, 33.6, 11.1; **HRMS** (ESI)  $m/z$ :  $[\text{M}+\text{H}]^+$  calculated 235.0925, found 235.0923. [Figures S9I](#) and [S9J](#).

#### **QUANTIFICATION AND STATISTICAL ANALYSIS**

This study does not involve quantification and statistics.

#### **ADDITIONAL RESOURCES**

This work is not part of a clinical trial.